NATIONAL ADVISORY COMMITTEE FOR AERONAUTICS

TECHNICAL NOTE

No. 1494

A METHOD FOR ESTIMATING HEAT REQUIREMENTS FOR ICE PREVENTION ON GAS-HEATED HOLLOW PROPELLER BLADES

By V. H. Gray and R. G. Campbell

Flight Propulsion Research Laboratory
Cleveland, Ohio

Washington
December 1947

NATIONAL ADVISORY COMMITTEE FOR AERONAUTICS

TECHNICAL NOTE NO. 1494

A METHOD FOR ESTIMATING HEAT REQUIREMENTS FOR ICE PREVENTION ON GAS-HEATED HOLLOW PROPELLER BLADES

By V. H. Gray and R. G. Campbell

SUMMARY

A detailed method is presented for determining the temperature and flow of heated gas necessary for ice prevention of hollow propeller blades in flight and icing conditions. The propeller blade is analytically divided into a number of short radial segments, which are successively treated as separate heat exchangers. Expressions for the total external and internal heat transfer are combined to determine the surface temperatures of each segment. The thermodynamic steady-flow equation is given for the internal gas-flow process and expressions are obtained for the radial variations of gas temperature and pressure within the blade. For a given initial gas temperature in the blade shank cavity, the minimum gas flow is determined, which will provide surface temperatures of at least 32° F everywhere on the heated portion of the blade.

An expression for the required heat-source input to the gas is included and a formula is given for calculating the required blade-tip nozzle area.

A discussion is included of the indicated benefits to be derived from certain alterations of the blade internal flow passage.

INTRODUCTION

Thermal prevention of the formation of ice on aircraft propellers has been previously investigated by means of electrical and hot-gas heating. The heat requirements associated with the use of external, electrically heated rubber blade shoes are analyzed in reference 1. Flight investigations of thermal systems using hot gas within hollow propeller blades have been reported in reference 2, and by Palmatier and Brigham of the Curtiss-Wright Corporation.

The present analysis was made at the NACA Cleveland laboratory to provide a method for predicting the hot-gas flow and the initial gas temperature required for satisfactory ice prevention on hollow propeller blades. This method involves a system of progressive approximations considering successive radially disposed blade segments as separate heat exchangers. Account is taken of the heat required to raise the temperature of the intercepted free water to the blade-surface temperature, the cooling effect of the evaporation of water, and the kinetic heating of the external-air boundary layer. The physical changes of the hot gas in flowing through the hollow blade are determined in order to find the required tip nozzle area. The detailed analysis is applied to a typical propeller blade for flight at two assumed operating conditions at the same icing conditions to illustrate the step-by-step procedure and to demonstrate typical results. A method of modifying the blade internal passage is suggested whereby the heating requirements may be reduced for a given application of the hot-gas method of preventing ice on typical hollow propellers.

SYMBOLS

The following symbols are used in equations taken from references:

A heat-transfer area, (sq ft)

A_n cross-sectional area of blade tip nozzle, (sq ft)

A_p cross-sectional area of blade internal-flow passage, (sq ft)

C_l blade-section lift coefficient

c blade chord, (ft)

c_n specific heat of gas for polytropic process, (Btu/(lb)($^\circ$F))

c_p specific heat of gas at constant pressure, (Btu/(lb)($^\circ$F))

D_c diameter of cylinder whose radius is equal to leading-edge radius of given blade section, (ft)

D_h hydraulic diameter, ($4 A_p/P$), (ft)

E_{1-2}	change of radial kinetic energy per pound of gas in flowing through radial blade segment, (ft-lb/lb)
e	base of natural logarithms
F_{1-2}	flow energy dissipated by friction per pound of gas in flowing through radial blade segment, (ft-lb/lb)
f	friction coefficient
g	acceleration of gravity, 32.2 (ft/sec^2)
H	rate of heat transfer per unit area, (Btu/(hr)(sq ft))
h	convective heat-transfer coefficient, (Btu/(hr)(sq ft)($^\circ$F))
J	mechanical equivalent of heat, (ft-lb/Btu)
k	thermal conductivity, (Btu/(hr)(sq ft)($^\circ$F/ft))
L	latent heat of evaporation of water, (Btu/lb)
l	radial length of blade segment, (ft)
M	rate of interception of water, (lb/(hr)(sq ft))
M_{ev}	rate of evaporation of water, (lb/(hr)(sq ft))
m	liquid-water content of ambient air, (grams/cu m)
Nu	Nusselt number, ($h\delta_l/k$ or $h\delta_t/k$)
n	exponent in polytropic process, pv^n = constant
P	perimeter of blade internal-flow passage, (ft)
Pr	Prandtl number, (3600g) $\mu c_p/k$
p	absolute static pressure, (lb/sq ft)
p_v	pressure of saturated water vapor, (lb/sq ft)
Q_I	heat input to gas flow per blade from heat source, (Btu/hr)
Q_n	heat escape per blade at tip nozzle, (Btu/hr)
Q_T	total heat added per blade to internal gas flow from heat source and propeller work, (Btu/hr)

Q_{trans} heat transferred through blade metal from gas flowing through radial blade segment, (Btu/hr)

Q_{1-2} net heat loss per pound of gas in flowing through radial blade segment, $\frac{Q_{trans}}{W} - \frac{F_{1-2}}{J}$, (Btu/lb)

q dynamic pressure of ambient air relative to blade station, (lb/sq ft)

R gas constant (for air = 53.3), (ft-lb/(lb)($^{\circ}$R))

Re_c Reynolds number based on blade-section chord

$Re_{D,h}$ Reynolds number based on hydraulic diameter

$Re_{\delta,l}$ Reynolds number based on laminar boundary-layer thickness

r radius at any propeller-blade station, (ft)

s_T surface total length of heated blade section in chordwise direction over both camber and thrust face, (ft)

s surface distance from blade-section stagnation point to any point on heated surface in chordwise direction, (ft)

T absolute total temperature, ($^{\circ}$R)

t static temperature, ($^{\circ}$F)

Δt temperature rise at surface due to boundary-layer friction, ($^{\circ}$F)

U internal energy of gas, (Btu/lb)

u_r radial velocity of internal gas relative to propeller blade, (ft/sec)

u_t tangential velocity of propeller blade at given radius, (ft/sec)

V air velocity, (ft/sec)

V_{av} average air velocity over camber or thrust face of blade, (ft/sec)

V_R resultant or helical velocity of propeller blade at any radius, (ft/sec)

v	specific volume of internal gas, (cu ft/lb)
W_{prop}	increment of enthalpy due to work done by rotating propeller on pound of gas in flowing through radial blade segment, (ft-lb/lb)
W_{1-2}	net compression work done on pound of gas in flowing through radial blade segment, $W_{prop} - F_{1-2}$, (ft-lb/lb)
w	rate of internal gas flow per blade, (lb/hr)
X	Hardy's evaporation factor
x	distance from leading edge measured along chord, (ft)
Z	exponent of Pr in determining kinetic temperature rise, 1/2 for laminar flow and 1/3 for turbulent flow
α	angle of attack of blade section, (deg)
γ	ratio of specific heats
δ_l	thickness of laminar boundary layer on blade surface, (ft)
δ_t	heat-transfer length of turbulent boundary layer, (ft)
ϵ	momentum thickness of boundary layer on blade surface at transition, (ft)
ζ	turbulent boundary-layer parameter
ζ_{tr}	turbulent boundary-layer parameter at point of transition
λ	propeller drive-shaft torque increment due to internal gas flow, (lb-ft/(lb/sec))
μ	absolute viscosity, ((lb)(sec)/(sq ft))
υ	kinematic viscosity, (sq ft/sec)
ρ	density, $((lb)(sec^2)/ft^4)$
τ	static temperature, (^oR)
τ_y	arithmetic average of static temperatures of ambient air and blade surface, (^oR)
ϕ	angular position relative to stagnation point on blade-section leading-edge circular arc, (deg)

ψ angle of impingement of water droplet on blade surface, (deg)

ω propeller rotational speed, (radians/sec)

Subscripts:

0 ambient atmospheric conditions

1, 2 internal gas at entering and leaving ends, respectively, of a given radial segment

a external air side of propeller blade

av average

b outer edge of external-air boundary layer

d datum temperature (for determining heat-transfer differentials)

f final gas conditions (exit from last radial blade segment prior to tip nozzle)

g internal gas side of propeller blade

i initial gas condition (inlet to first radial blade segment)

m mean value between points 1 and 2

s external blade surface

w occurrence of condensation or evaporation of water

Primed symbols denote conditions that are changed because of altered blade interiors.

METHOD FOR DETERMINING DESIGN REQUIREMENTS

Description of Solution

The determination of the required gas-flow rates for a hot-gas type of anti-icing system on a given aircraft propeller involves a tedious series of calculations. The information available at the present time is insufficient to determine

quickly the maximum requirements for a given propeller operating through a range of flight and icing conditions. Individual calculations must be made for a complete series of selected, critical flight and icing conditions. The blade-tip nozzle area and the heat-source capacity are then calculated for the maximum requirements so determined.

The degree of approximation obtained through the use of the subsequent analysis will remain uncertain until more complete and reliable experimental data are available on propeller-blade external and internal heat-transfer coefficients, kinetic heating of wet air, heat losses due to evaporation of water, the extent of heat conduction in the blade metal, and the determination of minimum standards for ice prevention.

A schematic diagram of the heated-gas flow through a typical hollow propeller blade is illustrated in figure 1. The gas is first heated by a suitable heat source, enters a stationary transfer manifold, and then passes through a collector ring and cuffs fastened to the propeller hub and into the blade shanks. The hot gas then flows radially outward through the hollow blades, which may have internal radial partitions (fig. 1), to discharge nozzles in the blade tips.

The method suggested starts with the selection of a number of operating conditions (propeller rotational speed, airspeed, density altitude, and ambient-air temperature) characteristic of taxiing, take-off, climb, cruise, and maximum speed with the determination of the corresponding liquid-water contents from the recommendations shown in figure 2. The required internal hot-gas flow is then calculated for each condition using an initial hot-gas temperature as high as structural considerations will permit.

For some flight conditions the required internal gas flow obtained in the calculations using the maximum initial gas temperature will be so low that a reduction in the initial temperature and an increase in the gas flow might seem advisable. In many cases, however, the maximum heat requirements will probably be met only by utilizing the highest possible initial hot-gas temperature because of limitations of the propeller in pumping the gas. The use of high gas temperatures and low gas flows has the additional advantage of keeping the pumping power at a minimum.

The required gas flow, which is defined as the rate that will maintain the heated portion of a blade surface at temperatures at or above 32° F, must be computed by trial. For conventional

propeller-blade designs, the point of lowest calculated surface temperature will usually be at the stagnation point of a radial station near the hub. Under severe icing conditions, there is no great variation of calculated leading-edge surface temperature with propeller radius at the inboard stations, although heat conducted radially outward from the blade hub will actually raise the surface temperatures at the inner radii. If the effect of this heat conduction from the blade shank does not extend too far along the blade at the leading edge, the use of the stagnation-point surface temperature at the innermost blade segment as the critical point for determining the required gas flow will permit more rapid progression with the trial values and seldom will a complete analysis of all segments be necessary.

Steps in Solution

For each set of flight and icing conditions the following step-by-step method of solution is suggested.

I. Divide the blade into a convenient number of radial segments each l long. (In the numerical example given subsequently, radial segments 1 ft long were employed; experience may indicate a need for shorter segments of perhaps 6 in. in length.) Tabulate the cross-sectional flow areas A_p, the external and internal heat-transfer areas A_a ($= s_T l$) and A_g ($= Pl$), respectively, the diameters of equivalent leading-edge cylinders D_c at the centers of the segments, the internal perimeters P, and the chord lengths c. The cross-sectional flow areas should be tabulated for the inlet, the center, and the outlet of each segment.

II. Determine the external factors that are unaffected by the internal heat flow as follows: For the assumed propeller-blade speed, find the lift coefficient C_l and angle of attack α at the center of each radial segment by the method of reference 3 or other accepted procedure. With these data calculate the chordwise distribution of local air velocity V_b.

A. Determine the local external air-film heat-transfer coefficient h_a for the laminar regime (from reference 4) from

$$h_a = \frac{Nu\ k}{\delta_l} \tag{1}$$

where the value of the laminar boundary-layer thickness δ_l is found from reference 5 as

$$\delta_l^2 = \frac{5.3\ c^2}{Re_c}\left(\frac{V_R}{V_b}\right)^{9.17}\int_0^{s/c}\left(\frac{V_b}{V_R}\right)^{8.17} d\left(\frac{s}{c}\right) \qquad (2)$$

For the turbulent regime the heat-transfer coefficient has been given in reference 6 as

$$h_a = \frac{Nu\ k}{\delta_t} \qquad (3)$$

The value of the turbulent boundary-layer heat-transfer length δ_t is slightly involved. The turbulent boundary-layer parameter ζ, as derived in reference 7, is related to δ_t as follows:

$$\delta_t = \frac{\zeta^2\ c}{Re_c\ \frac{V_b}{V_R}} \qquad (4)$$

The value of the parameter ζ, denoted ζ_{tr} at the transition point (appendix A), is given in reference 7 as

$$\zeta_{tr} = 2.56\ \log_e 4.075\frac{V_b\ \epsilon}{\upsilon} \qquad (5)$$

where

$$\epsilon = 0.289\ \delta_l \qquad (6)$$

the value of δ_l being taken at the transition point. Succeeding values of ζ may be found from the relation

$$\frac{d\zeta}{dx} + \frac{6.13}{V_b}\frac{dV_b}{dx} = \frac{V_b}{\upsilon}\,f(\zeta) \qquad (7)$$

where the function $f(\zeta)$ is

$$f(\zeta) = 10.411\ \zeta^{-2}\ e^{-0.3914\zeta} \qquad (8)$$

An alternate and simpler method than that above for determining h_a (explained in appendix A) is given in reference 8 as

$$h_a = 0.0582 (\tau_y)^{0.50} \left(\frac{V_{av} \rho_0 g}{s}\right)^{0.50} \quad (9)$$

for the laminar regime, and

$$h_a = 0.524 (\tau_y)^{0.296} \left(\frac{V_{av} \rho_0 g}{s^{0.25}}\right)^{0.80} \quad (10)$$

for the turbulent regime, where

$$V_{av} \approx V_R \left(1 \pm \frac{C_l}{4 \cos \alpha}\right) \quad (11)$$

The + is used for the camber surface and the - is used for the thrust face. Inasmuch as the values of h_a in equations (1), (3), (9), and (10) cannot be determined at the stagnation point, determine values of h_a near the leading edge (appendix A) from the equation of reference 8

$$h_a = 0.194 (\tau_y)^{0.49} \left(\frac{V_R \rho_0 g}{D_b}\right)^{0.50} \left(1 - \left|\frac{\phi}{90}\right|^3\right) \quad (12)$$

B. Determine the rate of water interception M (appendix B) from

$$M = \frac{m}{4.45} V_R \sin \psi \quad (13)$$

C. Determine the local heat-transfer datum air temperature $t_{a,d}$ (appendix B) from

$$t_{a,d} = t_{b,w} + \Delta t_{a,w} \quad (14)$$

for saturated air flowing over a wet surface. If the air flowing over the surface is unsaturated, the

local air temperature at the outer edge of the boundary layer becomes t_b, and if the surface is dry the air-temperature rise in the boundary layer due to friction becomes Δt_a. The values of $t_{b,w}$ and t_b are determined from the adiabatic compression lines, shown in figure 3, plotted from data of reference 9. From the intersection point of the ambient-air temperature t_0 and pressure p_0, determine the proper adiabatic line; then the local temperature at the outer edge of the boundary layer t_b at any point over the airfoil is found by following this adiabatic line parallel to those shown to the local pressure p_b, given by

$$p_b = p_0 + q\left[1 - \left(\frac{V_b}{V_R}\right)^2\right] \tag{15}$$

The values of Δt_a and $\Delta t_{a,w}$ have been developed in reference 10 as follows;

$$\Delta t_a = \frac{V_b^2 \, Pr^Z}{2gJc_p} \tag{16}$$

and

$$\Delta t_{a,w} = \Delta t_a - 0.622 \frac{L}{c_p}\left(\frac{p_{v,a} - p_{v,b}}{p_b}\right) \tag{17}$$

where the saturated vapor pressures $p_{v,a}$ and $p_{v,b}$ correspond to the temperatures $t_{a,d}$ and t_b, respectively, necessitating a solution of $\Delta t_{a,w}$ by trial at each point.

III. In order to determine the changes in the internal gas flow through the blade, select the desired inlet-gas temperature $t_{g,i}$, which equals $t_{g,1}$ for the first radial segment, and a trial value of hot-gas flow w.

A. Assume the temperature of the gas leaving the first segment $t_{g,2}$.

1. Determine the internal gas-film heat-transfer coefficient h_g (appendix C) from reference 11

$$h_g = 4.1 \times 10^{-4} \frac{(\tau_{g,m})^{0.3} \, w^{0.8} \, p^{0.2}}{A_p} \tag{18}$$

using

$$\tau_{g,m} = \frac{\tau_{g,1} + \tau_{g,2}}{2} \tag{19}$$

2. Determine the mean heat-transfer datum gas temperature for the segment $t_{g,d}$ from

$$t_{g,d} = t_{g,m} + \Delta t_g = t_{g,m} + \frac{(u_{r,m})^2 \, Pr^{0.33}}{2gJc_p} \tag{20}$$

where

$$u_{r,m} = \frac{W}{A_p} \frac{R}{3600} \frac{(\tau_{g,m})}{p_{g,m}} \tag{21}$$

For the first estimate of $t_{g,2}$, let $p_{g,m} \approx p_{g,1}$; for subsequent trials let

$$p_{g,m} \approx \frac{p_{g,1} + p_{g,2}}{2}$$

of the preceding trial. (Details for calculating $p_{g,2}$ will be presented subsequently.) As the solution is approached this error will become very small.

3. Determine the chordwise distribution of surface temperature t_s (appendix C) at the center of the segment from

$$t_s = \frac{h_g t_{g,d} A_g + \left[h_a X t_{a,d} + M \left(t_0 + \frac{V_R^2}{2gJ} \right) \right] A_a}{h_g A_g + (h_a X + M) A_a} \tag{22}$$

where (see appendix B)

$$X = 1 + \frac{p_{v,s} - p_{v,a}}{t_s - t_{a,d}} \left(\frac{0.622\ L}{p_b\ c_p} \right) \tag{23}$$

and $p_{v,s}$ and $p_{v,a}$ correspond to the temperatures t_s and $t_{a,d}$, respectively, for a wet surface. Because X varies with t_s, the values of t_s at each point must be computed by trial.

4. In order to determine the heat transferred through the blade metal of the segment, plot $(t_{g,d} - t_s)$ against s/c for the chordwise extent of the heated surface and obtain the average value by graphical integration or by Simpson's rule. The heat transferred through the blade metal Q_{trans} is then

$$Q_{trans} = (t_{g,d} - t_s)_{av}\ h_g A_g \tag{24}$$

5. Determine the energy change due to friction in the segment F_{1-2} per pound of gas flow (from reference 12)

$$F_{1-2} = \frac{u_{r,m}^2}{2g} \frac{l}{D_h} f \tag{25}$$

where

$$f = 0.0056 + \frac{1}{2} (Re_{D,h})^{-0.32} \tag{26}$$

and

$$Re_{D,h} = \frac{w\ D_h}{A_p\ \mu_{g,m}\ (3600\ g)} \tag{27}$$

6. Determine the polytropic specific heat of gas c_n from

$$Q_{1-2} = \frac{Q_{trans}}{w} - \frac{F_{1-2}}{J} = c_n\ (t_{g,1} - t_{g,2}) \tag{28}$$

and the polytropic exponent n from

$$n = \frac{c_p - c_n}{\frac{c_p}{\gamma} - c_n} \tag{29}$$

7. Determine the pressure of the gas leaving the segment $p_{g,2}$ from

$$p_{g,2} = p_{g,1}\left(\frac{\tau_{g,1}}{\tau_{g,2}}\right)^{\frac{n}{1-n}} \tag{30}$$

where $p_{g,1}$ is estimated for a particular hot-gas-flow system from published experimental pressure-loss data on ducts and manifolds. Find the change in radial kinetic energy E_{1-2} per pound of gas flow through the segment from

$$E_{1-2} = \frac{u_{r,2}^2 - u_{r,1}^2}{2g} = \frac{w^2}{(3600)^2\,(2g^3)}\left[\left(\frac{1}{A_{p,2}\,\rho_{g,2}}\right)^2 - \left(\frac{1}{A_{p,1}\,\rho_{g,1}}\right)^2\right] \tag{31}$$

8. Determine the net compression work W_{1-2} (appendix D) done on each pound of gas in flowing through the segment from

$$W_{1-2} = W_{prop} - F_{1-2} = \frac{u_{t,2}^2 - u_{t,1}^2}{2g} - F_{1-2} \tag{32}$$

9. Finally, check the accuracy of the assumed $t_{g,2}$ (appendix D) from

$$t_{g,1} - t_{g,2} = \left[\frac{\gamma - n}{(\gamma - 1)\,nJc_n}\right](W_{1-2} - E_{1-2}) \tag{33}$$

and reestimate $t_{g,2}$ until the value obtained from equation (33) agrees with the initial estimate in step III-A.

B. For the subsequent radial segments, repeat step III-A using the values of $t_{g,2}$ and $p_{g,2}$ of one segment as $t_{g,1}$ and $p_{g,1}$, respectively, of the next segment.

C. If t_s at any point (found in step III-A-3 for the correct $t_{g,2}$) proves to be less than 32° F, it can be increased by increasing the hot-gas flow w and repeating step III. Usually t_s will be a minimum at the stagnation point and at a segment near the hub.

IV. From the final conditions of the gas leaving the last segment, determine the tip nozzle area A_n required to maintain the gas flow (for unity discharge coefficient) from

$$A_n = \frac{w R \sqrt{T_{g,f}}}{3600\, p_0 \sqrt{2gJc_p \left(\frac{p_{g,f}}{p_0}\right)^{\frac{\gamma-1}{\gamma}} \left[\left(\frac{p_{g,f}}{p_0}\right)^{\frac{\gamma-1}{\gamma}} \left(\frac{T_{g,f}}{T_{g,f}}\right) - 1\right]}} \tag{34}$$

where

$$T_{g,f} = (T_{g,f}) + \frac{u_{r,f}^2}{2gJc_p} \tag{35}$$

V. Calculate the following: The required input from the heat-source Q_I, excluding losses in the induction system prior to the initial point, from

$$Q_I = w\, c_p\, (T_{g,i} - T_0) - \frac{w}{J} \frac{u_{t,i}^2}{2g} \tag{36}$$

the total heat added to the gas flow Q_T from

$$Q_T = Q_I + \frac{w}{J} \frac{u_{t,f}^2}{2g} \tag{37}$$

the heat escape at the tip nozzle Q_n from

$$Q_n = w\, c_p\, (T_{g,f} - T_0) \tag{38}$$

and the heat transferred through the entire heated surface of the blade ΣQ_{trans} from

$$\Sigma Q_{trans} = Q_T - Q_n = w\, c_p\, (T_{g,i} - T_{g,f}) + \frac{w}{J}\left(\frac{u_{t,f}^2 - u_{t,i}^2}{2g}\right) \tag{39}$$

Thus, the effectiveness of the propeller blade as a heat exchanger is given by $\frac{\Sigma Q_{trans}}{Q_T}$.

NUMERICAL EXAMPLES

Flight and Icing Conditions

The procedure for determining the design requirements for a gas-heated propeller has been applied to a theoretical hollow steel propeller having blades with central radial ribs, as shown in figure 1. The propeller-blade-form characteristics are given in figure 4 and other pertinent data in table I. An assumption has been made that heated air enters the blade shanks from a collector ring through suitable orifices and passes radially outward through only the leading-edge cavity in the blades, as illustrated in figure 1. The blade was arbitrarily divided for convenience into four radial segments each 1 foot long starting at the 18-inch station. The radial stations for which the surface-temperature calculations were made were therefore at 24, 36, 48, and 60 inches. (See fig. 4.) For more accurate results calculations nearer the hub may be necessary. A greater number of shorter radial segments may also be needed in regions where either the blade airfoil section or the internal flow area changes rapidly with radius.

For purposes of comparison, the calculations have been made for the two following operating conditions through the same icing condition:

Condition	A	B
Pressure altitude, ft	18,000	18,000
Ambient-air temperature, °F	0	0
True flight speed, mph	400	325
Propeller speed, rpm	1430	800
Liquid-water content, g/cu m	0.4	0.4

The value of liquid-water content chosen was based on the recommendations shown in figure 2.

For convenience in determining the initial internal gas conditions at the blade shanks, an arbitrary assumption was made that the internal static pressure in the blade shanks would be the ambient atmospheric pressure plus three-fourths of the flight dynamic pressure. The assumed hot-gas flow was varied at an initial temperature of 500° F until surface temperatures of 32° F or more were obtained over the heated surface of the blade.

Results

The general results are summarized as follows:

Condition	A	B
Gas flow per blade, lb/hr	450	750
Initial gas temperature, °F	500	500
Final gas temperature, °F	349.6	320.8
Heat-source input required per blade, Btu/hr	50,550	86,680
Required blade-tip nozzle area, sq ft	0.00466	0.0132

The results of the calculations are given in more detail in table II and figures 5 to 10. For the four radial stations and for both simulated flight conditions, the chordwise variation of local velocity ratio V_b/V_R is shown in figure 5; the external heat-transfer coefficient h_a is shown in figure 6; the local water interception M and evaporation M_{ev} rates are shown in figure 7; the local heat-transfer datum temperature $t_{a,d}$ is shown in figure 8; and the external-surface temperature t_s is shown in figure 9. The radial distributions of internal gas temperature t_g, internal gas pressure p_g, internal heat-transfer coefficient h_g, and the external-surface temperature at the stagnation point t_s are shown in figure 10 for conditions A and B.

The calculations of the external heat-transfer coefficients were made using equations (1), (3), and (12). Attempts were made to locate accurately the external boundary-layer transition points using the methods of references 13 and 14, and the theoretical transition points were found to be located aft of the heated

areas. In four cases the velocity distributions (fig. 5) have fairly distinct peaks near the leading edge and an arbitrary assumption was made that the surface roughness due to the impinging water would cause transition at these minimum-pressure points. This assumption applies to the camber face at the 48-inch station for condition A and to the thrust face at the 60-inch station and the camber face at the 36- and 48-inch stations for condition B. The resulting chordwise distributions of h_a, shown in figure 6 for these cases, are similar to the type shown on the left side of figure 11 and discussed in appendix A, inasmuch as in each case the transition point occurs very close to the leading edge.

The surface temperatures are obtained from equation (22), in which the external heat-transfer area A_a is arbitrarily assumed to extend aft of the blade-rib center line for a distance on each face equal to half the maximum blade thickness. This assumption is to account approximately for the heat transfer to the trailing half of the blade, which in reality diminishes all the way to the trailing edge. An unpartitioned blade would not require such an approximation.

DISCUSSION

Thin-Skin Approximation

The largest source of error in this analysis is thought to be the thin-skin approximation used in the solution of external surface temperatures. This approximation makes use of two related assumptions. First, the value of H_g depends on the temperature differential $(t_{g,d} - t_s)$, in which the temperature gradient through the blade metal is assumed to be zero. This gradient and the error involved is usually small, except at the leading-edge region, for any propeller blade made of steel or metal with equal or higher thermal conductivity. Second, the heat balance employed in equation (22) is based on the assumption that the total heat transfer from the internal gas to the external air can be considered to be distributed uniformly and to pass only normally through suitable internal and external heat-transfer areas; that is, the blade metal is assumed to be infinitely thin and surfacewise heat conduction is neglected. The ratio of the two heat-transfer areas is then used to determine the ratio of the local internal and external heat-transfer rates. The error involved in this assumption is thought to be large inasmuch as the thermal conductivity of the blade metal is usually very high compared

with the conductivity through the gas and air surface films. Surfacewise heat conduction within the blade metal is certain to reduce the temperature gradients indicated by the variations of surface-film heat-transfer coefficients and changes in metal thickness.

The two foregoing errors can be eliminated from the analysis if the blade segments are studied using the "relaxation" method developed in reference 15. No attempt has been made to use this method because of the prodigious amount of time and effort involved. The method and a sample of the results to be expected from it are given in appendix E.

Principal Factors Affecting Heat Requirements

From a consideration of the foregoing analysis and the numerical examples, the required internal heat flow through hollow propellers depends on the following factors external to the blade surface, which appear to have the largest effects in determining the local heat transfer through the metal necessary to prevent ice.

Ambient temperature. - With other factors remaining constant, the heat transfer through the blade surface required for ice prevention as defined herein varies directly with the temperature difference between the freezing temperature and the datum temperature (ambient temperature plus kinetic increment). Even though the assumed liquid-water content of the ambient air decreases with decreasing temperatures, the heat required to maintain a minimum surface temperature of 32° F steadily increases as ambient temperature decreases; but, computed on the basis of immediate evaporation of all the water that strikes the surface, the heat required will decrease with decreasing temperatures because the liquid-water content decreases. The point at which the heat requirements are equal when computed on both bases of heating represents the maximum possible value of heat required. This maximum value represents excessive heating for the conditions used in the examples presented.

Water impingement. - An increase in the rate of water interception requires a direct increase in the amount of heat required to raise its temperature above 32° F. A more important factor, when external heat requirements are considered, is that an increase in the rate of water interception increases the amount of runback, which increases the area of wetted surface and thus requires more heat to offset the evaporative heat loss. The difference in temperatures between a wet and a dry surface resulting from the same

internal heat flow can be observed in figure 9(b), where the surface becomes dry on the thrust face of both the 48- and 60-inch stations. The surface-temperature rise above ambient temperature more than doubles its value in the two instances after the surface becomes dry.

Kinetic heating. - Kinetic heating always reduces the heat requirements for ice prevention because it increases the heat-transfer datum temperature above the ambient temperature. Its temperature rise increases as the square of the resultant velocity and has a lower value in wet air than in dry air. This increment of temperature becomes important as a saving in required heat flow at high resultant velocities of the order shown in the two examples presented. A fact of interest is that heat requirements are reduced according to the square of the resultant velocity (because of kinetic heating) and are also increased according to the square root of the resultant velocity (because of the heat-transfer coefficient). The net result is that as velocity is increased the heat required to maintain a surface temperature of 32° F first increases and then decreases; the location of the maximum heat requirement depends on the conditions involved. This maximum heat requirement probably occurs below a velocity of 400 feet per second for most conditions. Thus, except for other variations (such as changes in propeller-blade sections), the heat requirements for propellers on high-speed airplanes are usually greatest at the inboard stations. For the same reason, the heat requirements are reduced by increasing the rotational speed of the propeller.

Location of transition. - The determination of heat transfer from a propeller blade depends to a large extent on the exact location of transition. As shown in figure 11, considerably more heat transfer results over the blade faces for which turbulent flow is assumed (as shown by the higher heat-transfer coefficients) than would be the case if laminar flow were assumed. The same result is shown in figure 9, in which the low surface temperatures of the four faces under assumed turbulent flow indicate a higher rate of heat transfer. Of course, transition might be caused by water-film roughness on many of the surfaces for which laminar flow was assumed, because the velocity gradients are quite low over all the stations, as shown in figure 5.

Altitude. - The altitude-pressure term frequently appears in the analysis and its total effect on heat requirements is difficult to evaluate. The two principal effects of altitude (other factors remaining constant) on the required blade-metal heat transfer are largely compensatory. With increasing altitude the heat transfer due to the evaporation processes increases whereas the heat transfer

due to external convection decreases. Increasing altitudes have a serious effect on restricting the internal gas flow. In order to offset the reduction in gas density with altitude, the gas flow w must be maintained by increasing the internal gas velocity, with resulting increases in flow friction and pressure drop. These increases, coupled with the loss of ram pressure at altitude, indicate that the required internal gas flow steadily becomes more difficult to maintain with increasing altitude and that a booster pump may be necessary at high altitudes to attain the required gas flow. A pressure boost can also be obtained by increasing the propeller rotational speed whenever possible.

Comparison of Results of Numerical Examples

Flight condition B required a larger internal heat flow than condition A for two reasons: the kinetic heating was less, owing to a lower airspeed and propeller speed, and the surface area under assumed turbulent flow was greater.

The required tip nozzle area for condition B was almost as large as the internal flow area at the exit to station 60, which indicated that the gas pressure at the tip had dropped nearly to its lowest limit and that a higher rate of flow was almost impossible without augmenting the initial gas pressure or increasing the propeller speed. If this tip nozzle area is used, the flow will become excessive under conditions of higher airspeed and propeller speed or lower altitude. The hot-gas flow could, however, be regulated by a throttle in the intake system.

The required heat-source capacities for these two conditions appeared to be very high compared with external electrically heated blade shoes based on the meager experimental data available. The high required heat-source input is, however, explained by the fact that internal gas-heating systems normally have no selective control of heat transfer and as a result much of the surface area is considerably overheated and further wastage occurs at the tip nozzle. In the examples that used this method of blade heating, only a narrow band at the leading-edge surface had temperatures near 32° F. Consequently, if a narrow strip of ice 0.3 inch wide, for example, were to be permitted along the leading edge, the internal heat-flow requirement for station 24, condition B, (most critical) would be nearly halved. This reduction would result because the surface temperature at the stagnation point could then be allowed to drop approximately 9° below 32° F and the differential $(t_s - t_{a,d})$ would be approximately one-half its original value (17.6° F). Because

the stagnation point is the controlling factor for the segment, the internal heat flow could then be reduced by nearly half and the blade-surface temperatures would remain above 32° F except for the narrow leading-edge band. In practice, the internal heat flow required therefore depends largely on whether narrow strips of ice along the leading edges are tolerated.

Suggested Technique for Reducing Heat Flows

A method of reducing the required heat flow in a typical hollow propeller blade is suggested in which the internal flow passage is altered to attain a more economical distribution of heat transfer. When it is assumed that equation (18) and the hydraulic diameter concept can be applied to internal passages whose perimeters contain convolutions, designs of flow passages can be developed whereby large reductions in heat-source capacity and pumping-power output are apparent over the typical hollow-blade interior, as shown in figure 1. Two suggested alterations are shown in figure 12 and compared with the original blade section. Using primes to denote the altered designs, the following mathematical comparisons can be shown:

For both the original and altered designs

$$h_g A_g = \frac{4.1 \times 10^{-4} \left(\tau_{g,m}\right)^{0.3} w^{0.8} P^{0.2} A_g}{A_p}$$

from equation (18). For the same inlet gas temperatures, assuming $P = A_g$ and taking the ratio of a modified design to the original design

$$\frac{(h_g A_g)'}{h_g A_g} \approx \left(\frac{w'}{w}\right)^{0.8} \left(\frac{A_g'}{A_g}\right)^{1.2} \left(\frac{A_p}{A_p'}\right)$$

Setting this ratio equal to unity will permit evaluation of the flow ratio that will produce the same amount of blade-surface heat-transfer as the original design, or

		Modification 1	Modification 2
$\frac{w'}{w} \approx \left(\frac{A_g}{A_g'}\right)^{1.5} \left(\frac{A_p'}{A_p}\right)^{1.25}$	$\approx$	0.149	0.152

As

$$u_r = \frac{w}{A_p \rho g (3600)}$$

$\frac{u_r'}{u_r} \approx \left(\frac{A_g}{A_g'}\right)^{1.5} \left(\frac{A_p'}{A_p}\right)^{0.25}$	$\approx$	.298	.228

As

$$F_{1\text{-}2} \sim u_r^{1.68} (D_h)^{-1.32}$$

$\frac{F_{1\text{-}2}'}{F_{1\text{-}2}} \approx \left(\frac{A_g}{A_g'}\right)^{1.20} \left(\frac{A_p'}{A_p}\right)^{-0.90}$	$\approx$	.813	.481

In summarizing these modifications, if the area of the internal flow passage is reduced and the internal heat-transfer area is increased, the same total heat transfer to the external surface can be maintained while the internal-gas flow is greatly reduced, A reduction of the flow lowers the internal velocity and the friction loss and thus raises the available internal pressure. When the flow is reduced, more heat is removed per pound of gas flow and, consequently, the gas temperature falls more rapidly and reduces the heat loss at the tip nozzle. Care should be taken with the internal heat-transfer area that some segments do not abstract such heat as to starve subsequent segments.

In addition to the foregoing reduction of heat flow, a better distribution of chordwise surface heat transfer can be accomplished by making the greatest increase of internal heat-transfer area at the leading edge by the use of fins similar to those shown in figure 12. An accurate determination of the magnitude of the heat transfer resulting from these modifications requires that the whole problem be approached along the lines of the relaxation method as outlined in appendix E. All the indications shown lead to the belief that a hollow propeller blade can be designed with

modifications similar to those illustrated, which will efficiently provide ice protection with a heat flow of feasible proportions.

COMMENTS AND RECOMMENDATIONS

The method presented for estimating heat requirements for ice prevention on gas-heated hollow propeller blades provides integrated means for determining the design requirements for ice prevention on gas-heated hollow propeller blades operating in any selected condition. Several of the suggested simplifications and other short methods can be used where conditions do not require a rigorous treatment. Solutions by trial are occasionally required, which are admittedly inconvenient, but become fairly rapid with increased familiarity.

Substantiation of several formulas, upon which this method is based, by experimental measurements in actual icing conditions is recommended. A relaxation analysis of the whole propeller blade should be made to determine the effect of leading-edge internal ribs and the exact heat transfer normally, radially, and chordwise through the blade metal.

Flight Propulsion Research Laboratory,
National Advisory Committee for Aeronautics,
Cleveland, Ohio, June 27, 1947.

APPENDIX A

EXTERNAL HEAT-TRANSFER COEFFICIENTS

Airfoil coefficients based on boundary layer. - Several methods are available for calculating the local and average heat-transfer coefficients for the surfaces of airfoils (references 4, 16, 17, and 13). Local surface values for the heat-transfer coefficients on airfoils (equation (1)) are derived in reference 4, primarily on the basis of Reynolds' analogy between skin friction and heat transfer through laminar boundary layers, and an alternate form of Reynolds' analogy (equation (3)) is presented for the turbulent boundary-layer case in reference 16. These solutions are detailed because they take into account the variation of local air velocity and boundary-layer thickness over the airfoil surface. No account has been taken either in this analysis or in the references, however, of the unknown effect on the boundary-layer heat transfer of the heat addition to the boundary layer caused by a heated surface.

Empirical airfoil coefficients. - The methods of reference 8 (equations (9) and (10)) have been added as alternate solutions for h_a because they offer easier solutions by their use of average air velocities over the faces of the airfoils. These equations require a slight but adequate approximation for use in this analysis when determining the average temperature τ_y, because the surface temperatures are unknown. However, estimates of average surface temperatures involving errors of less than $1\frac{1}{2}$ percent of h_a can easily be made.

Leading-edge cylinder coefficients. - At the stagnation point the value of h_a cannot be determined in equations (1), (3), (9), and (10). The suggestion is made in reference 8 that the leading edge of an airfoil be regarded as an isolated cylinder in transverse flow for which heat-transfer data are available in reference 18. When these data are used and Nusselt's number at the stagnation point is expressed as a function of Prandtl number and Reynolds number, an empirical equation for the heat-transfer coefficient over the forward half of the equivalent leading-edge cylinder (equation (12)) is developed (reference 8). Figure 11 diagrammatically illustrates the suggested technique of fairing the distribution of heat-transfer coefficients over the leading-edge cylinder into the laminar- and turbulent-flow distributions for the rest of the airfoil in two typical configurations. On the

thrust face, transition is shown to occur close to the leading edge and the h_a curve is faired directly from the leading-edge values into the turbulent-flow curve. On the camber face, transition is shown to occur after a length of laminar flow and the curve is arbitrarily faired into the turbulent regime. The former type of distribution occurs in the numerical example, in certain cases on both faces of the blade.

Location of transition. - In the foregoing considerations, the location of the transition point must be determined. For increasing local pressures, the point of transition, which may be assumed to be coincident with laminar separation, may be estimated by the method of references 13 and 14. For decreasing pressures, the suggestion is made in reference 5 that the Reynolds number based on the laminar boundary-layer thickness $Re_{\delta,l}$ at the point of transition is between the limits of 8000 and 9500.

The location of the transition point greatly affects the heat transfer from an airfoil because the heat-transfer coefficient for turbulent flow is considerably larger than that for laminar flow. No reliable method is known for predicting the point of transition when the airfoil is undergoing water impingement. The presence of water on the surface probably causes transition to occur forward of the point determined by the foregoing methods.

APPENDIX B

EFFECTS OF WETTED SURFACE

Rate of water interception. - The rate of water interception is only slightly overestimated by assuming that the droplets travel in straight-line paths intersecting the blade surfaces. This condition exists when the airfoil collection efficiency becomes 100 percent. Exact collection efficiencies for airfoils are unavailable, although fairly complete data are available for cylinders. For symmetrical and low-camber airfoils the use of existing data for cylinders whose diameters are equal or related to the leading-edge diameters of the airfoils can be made with a fair degree of approximation. Accordingly, propeller-blade-section leading-edge cylinders, under ordinary flight conditions, have collection efficiencies varying approximately from 80 percent near the hub to 98 percent near the tip. The error in assuming 100-percent collection efficiency for the propeller sections is not so great in figuring the rate of water interception as in determining the extent of wetted surfaces, as discussed in the succeeding section.

The local rate of water interception M is thus proportional to the sine of the angle ψ subtended by the relative wind (helical speed) vector and the tangent drawn to the blade surface at the point being considered. The value of M is given by equation (13).

Surface evaporation. - The effect of evaporation of water from the surface of an airfoil in increasing the heat transfer was first derived by Hardy (reference 19). He has presented an expression for a local evaporation factor X, which multiplies the local convective heat-transfer coefficient wherever the surface is wetted. This factor is given by equation (23) and the local rate of evaporation of water from the surface is given by

$$M_{ev} = \frac{h_a}{L} (X-1) (t_s - t_{a,d}) \qquad (40)$$

Where the local rate of evaporation is larger than the local rate of water interception, the surface will tend to become dry. If the blow-off of water from the surface is neglected, however, there will be runback of unevaporated water from the leading-edge region when the rate of intercepted water exceeds the rate of

evaporation. In this analysis the surface of the propeller-blade section is considered dry aft of the point s/c at which

$$\int_0^{s/c} M \, d(s/c) = \int_0^{s/c} M_{ev} \, d(s/c)$$

where the lower limit 0 is at the stagnation point. For a dry surface, X becomes 1 and no surface evaporation occurs.

Heat-transfer datum air temperature. - The heat-transfer datum temperature $t_{a,d}$ at any point on the blade surface is the surface temperature that would be obtained if the blade were a nonconducting unheated body. The value of $t_{a,d}$ is given by equation (14) based on figure 3 and equations (16) and (17). The nature of $t_{a,d}$ for a typical propeller blade operating in either saturated or unsaturated air is shown in figure 13. There are two components of $t_{a,d}$: the adiabatic temperature t_b or $t_{b,w}$ at the outer edge of the boundary layer and the temperature differential Δt_a or $\Delta t_{a,w}$ in the boundary layer due to kinetic friction. The frictional temperature rise in the boundary layer is slightly larger in turbulent flow than in laminar flow according to equations (16) and (17) (as the Prandtl number is raised to the one-third power in turbulent flow compared with the one-half power for laminar flow). Both the components of $t_{a,d}$ are affected by the presence of water. The frictional temperature rise in a boundary layer that remains saturated is less than the rise in an unsaturated boundary layer, due to evaporation. Likewise, the temperature at the edge of the boundary layer for a saturated air stream follows the saturated air adiabatic line.

Whether or not the air is saturated at a given point is often difficult to determine and, consequently, the determination of $t_{a,d}$ is uncertain. In this analysis the following course has been adopted: For a wet surface, which exists forward of the point where the accumulated water intercepted equals the accumulated water evaporated (as defined in the previous section)

$$t_{a,d} = t_{b,w} + \Delta t_{a,w} \qquad (14)$$

For a dry surface, which is assumed to begin abruptly aft of this point

$$t_{a,d} = t_{b,w} + \Delta t_a \tag{41}$$

Accordingly, only when the ambient air is unsaturated is

$$t_{a,d} = t_b + \Delta t_a \tag{42}$$

APPENDIX C

HEAT BALANCE

Local internal heat transfer. - The internal gas-film heat-transfer coefficient h_g is given by equation (18), which appears to be the most applicable formula for determining this coefficient. The equation is based on data obtained for fully developed turbulent flow in long tubes. It is doubtful, however, whether this equation will give satisfactorily accurate results when applied to flow through hollow propellers for two reasons: (1) The nonsymmetrical cross sections of a hollow propeller-blade passage and the effect on heat transfer of changes in flow area may not be fully accounted for in an equation based on flow in straight circular tubes; and (2) no account is taken in equation (18) of local flow variations along a plane normal to the direction of flow (chordwise in a propeller blade). In a rotating propeller, the Coriolis acceleration produces radial velocities along the leading edge of the internal passage that are higher than those toward the trailing edge. The local internal heat-transfer coefficient would therefore probably be higher at the leading edge than is indicated by the average value given by equation (18).

When the value of h_g given by equation (18) is used, the local internal heat transfer for a unit area can be written as

$$H_g = h_g (t_{g,d} - t_s) \tag{43}$$

where $t_{g,d}$ is the mean-flow static gas temperature plus the temperature rise due to surface friction (equation (20)).

Local external heat transfer. - The local rate of external heat transfer per unit area at any point may be expressed as

$$H_a = h_a X (t_s - t_{a,d}) + M c_m (t_s - t_0) - \frac{M V_R^2}{2gJ} \tag{44}$$

where c_m is the heat capacity of liquid water, taken herein as unity. The first term of equation (44) on the right-hand side gives the combined convective and evaporative heat transfer; the second term gives the sensible heat absorbed by the intercepted water during its temperature rise to the surface temperature; and

the third term gives the heat released by the impinging water at the expense of its kinetic energy. For simplicity, an approximate expression for H_a can be used, wherein

$$H_a = (h_a X + M)(t_s - t_{a,d}) \tag{45}$$

and the error in the approximation is small except at the leading edge where M is a maximum.

Heat-balance equation. - In this analysis the equilibrium of heat transfer to and from the blade surface at any point is expressed as

$$H_g \frac{A_g}{A_a} = H_a \tag{46}$$

When equations (43) and (44) are substituted in equation (46) t_s can be solved for:

$$t_s = \frac{h_g t_{g,d} A_g + \left[h_a X t_{a,d} + M\left(t_0 + \frac{V_R^2}{2gJ}\right)\right] A_a}{h_g A_g + (h_a X + M) A_a} \tag{22}$$

Equation (46) is based on the assumption that a thin-skin approximation can be used for determining the surface temperatures. (See section entitled "DISCUSSION.")

APPENDIX D

THERMODYNAMIC ANALYSIS OF GAS FLOW

Assumptions. - The method for determining the temperature and pressure of the internal gas during its flow through the hollow propeller blade is based on the thermodynamic steady-flow energy equation. The internal flow is assumed to have a uniform radial velocity distribution at any station. The assumption is made that for a short radial segment the polytropic exponent n of the internal flow process can be considered constant. The error involved will vary as the radial length l of the segments used in the solution. For convenience in using the polytropic relations for gas, the energy due to flow friction is assumed to be heat added to the gas at the expense of work done by the gas.

Analysis of flow process. - The thermodynamic steady-flow equation may be written in terms of the energies per pound of gas as

$$W_{1-2} - JQ_{1-2} = \frac{u_{r,2}^2 - u_{r,1}^2}{2g} + J(U_2-U_1) + (p_2v_2 - p_1v_1) \quad (47)$$

This equation states that the difference between the net compression work done on the gas and the net heat lost from the gas in passing through the segment is equal to the total of the differences between the kinetic, internal, and potential energies at the leaving and entering ends of the radial segment.

For a mechanically reversible process, the sum of all the mechanical-energy terms in equation (47) can be expressed by

$$E_{1-2} + (p_2v_2 - p_1v_1) - W_{1-2} \quad (48)$$

where E_{1-2} is defined as the radial kinetic energy term by equation (31). The net work for a polytropic process satisfying the relation pv^n = constant is given by

$$\frac{R}{n-1}(t_{g,1} - t_{g,2}) \quad (49)$$

and the flow work can be expressed as

$$p_2v_2 - p_1v_1 = R(t_{g,2} - t_{g,1}) \tag{50}$$

When equations (48) and (49) are equated and equation (50) is substituted, the net compression work becomes

$$W_{1-2} = E_{1-2} + \frac{n}{n-1} R(t_{g,2} - t_{g,1}) \tag{51}$$

In a similar manner, the internal-energy term of equation (47) can be written as

$$J(U_2 - U_1) = \frac{R}{\gamma-1} (t_{g,2} - t_{g,1}) \tag{52}$$

When equations (50), (51), and (52) are substituted, equation (47) becomes

$$Q_{1-2} = \frac{n-\gamma}{(1-n)(\gamma-1)} \frac{R}{J} (t_{g,2} - t_{g,1}) \tag{53}$$

However,

$$Q_{1-2} = \frac{Q_{trans}}{w} - \frac{F_{1-2}}{J} = c_n(t_{g,1} - t_{g,2}) \tag{28}$$

The gas-temperature differential through the segment can now be expressed in terms of the energy quantities by combining equations (51), (53), and (28) to obtain

$$t_{g,1} - t_{g,2} = \frac{\gamma-n}{(\gamma-1)\, nJc_n} (W_{1-2} - E_{1-2}) \tag{33}$$

In equation (33) the value of W_{1-2} is given by equation (32). The increment of enthalpy W_{prop} due to work done by the rotating propeller on a pound of gas in flowing through a radial segment is given by

$$W_{prop} = \frac{u_{t,2}^2 - u_{t,1}^2}{2g} \tag{54}$$

This equation can be shown as follows: The propeller-drive-shaft torque increment due to the internal gas flow through a blade

segment is given by the change in moment of tangential momentum, which may be written in terms of torque per pound of gas per second as

$$\lambda = \frac{r_2 u_{t,2} - r_1 u_{t,1}}{g} \tag{55}$$

where u_t is the blade tangential velocity at the radius r. The rate of work done on a pound of gas can be written as

$$\omega\lambda = \frac{(\omega r_2 u_{t,2} - \omega r_1 u_{t,1})}{g} = \frac{u_{t,2}^2 - u_{t,1}^2}{g} \tag{56}$$

because $u_t = \omega r$. For a straight rotating channel, the increase in tangential kinetic energy between two points is obviously given by

$$\frac{u_{t,2}^2 - u_{t,1}^2}{2g}$$

for a pound of gas, so the remainder of the total work represents the amount of external work done on a pound of gas in flowing through a radial segment to produce a change in the enthalpy of the gas.

APPENDIX E

EFFECT OF HEAT CONDUCTION THROUGH BLADE METAL AT LEADING EDGE

A study was made using the relaxation method as described in reference 16 to determine the effect of heat conduction in the blade skin on the temperature distribution around the leading edge. The original assumption that heat is transferred only in a direction normal to the blade skin, which was assumed to be infinitely thin, was expected to be appreciably upset by the variations of blade-metal thickness and of the effective external heat transfer around the leading edge.

Laplace's equation, which requires the reasonable assumption that the blade metal is a homogeneous, isotropic solid, was used with conditions at the internal boundary defined by

$$k \frac{d\theta}{dy} = h_g \theta \tag{57}$$

and at the external boundary by

$$k \frac{d\theta}{dy} = (h_a X + M)(\beta - \theta) \tag{58}$$

where

k	thermal conductivity of blade metal, Btu/(hr)(sq ft)($^{\circ}$F/ft)
θ	$(t_{g,d} - t_x)$, $^{\circ}$F
$t_{g,d}$	heat-transfer datum gas temperature, $^{\circ}$F
t_x	metal temperature (surface or internal), $^{\circ}$F
y	distance normal to boundary, ft
h_g	internal gas heat-transfer coefficient, Btu/(hr)(sq ft)($^{\circ}$F)
$(h_a X + M)$	effective external heat-transfer coefficient, Btu/(hr)(sq ft)($^{\circ}$F)

β $(t_{g,d} - t_{a,d})$, °F

$t_{a,d}$ heat-transfer datum air temperature, °F

The scale used was 1 inch = 0.05 inch and for convenience the solution was arbitrarily originated 1 inch in chord length from the leading edge. The metal temperatures at the starting points on both faces of the blade were assumed to be slightly less than the values of surface temperatures that were obtained in the numerical example. The inclinations of the isotherms to the surface at the starting points were estimated from the anticipated nature of the heat transfer. The values of metal temperature obtained are unreliable, but the isotherm and surface-temperature patterns obtained are believed indicative of the trends to be expected if the solution were to be extended over the entire blade cross section.

The calculated results obtained for simulated flight and icing condition B at the 24-inch station are shown in figure 14. Because heat is transferred everywhere within the metal normal to the isotherms, a considerable quantity of heat flows through the metal of the camber and thrust faces into the mass of metal at the leading edge, as shown in figure 14. The surface temperature distribution is changed and thus the surfacewise temperature gradients at the leading edge are greatly reduced. The surface temperature rise at the leading edge due to conduction in the metal is approximately as indicated by a comparison of the two curves at the bottom of figure 14.

REFERENCES

1. Scherrer, Richard: An Analytical Investigation of Thermal-Electric Means of Preventing Ice Formations on a Propeller Blade. NACA ACR No. 4H31, 1944.

2. Darsow, John F., and Selna, James: A Flight Investigation of the Thermal Performance of an Air-Heated Propeller. NACA TN No. 1178, 1947.

3. Bairstow, Leonard: Applied Aerodynamics. Longmans, Green and Co. (London), 2d ed., 1939, pp. 637-658.

4. Allen, H. Julian, and Look, Bonne C.: A Method for Calculating Heat Transfer in the Laminar Flow Region of Bodies. NACA RB, Dec. 1942.

5. Jacobs, E. N., and von Doenhoff, A. E.: Formulas for Use in Boundary-Layer Calculations on Low-Drag Wings. NACA ACR, Aug. 1941.

6. Frick, Charles V., Jr., and McCullough, George B.: A Method for Determining the Rate of Heat Transfer from a Wing or Streamline Body. NACA ARR, Dec. 1942.

7. Squire, H. B., and Young, A. D.: The Calculation of the Profile Drag of Aerofoils. R. & M. No. 1838, British A.R.C., 1937.

8. Martinelli, R. C., Guibert, A. G., Morrin, E. H., and Boelter, L. M. K.: An Investigation of Aircraft Heaters. VIII - A Simplified Method for the Calculation of the Unit Thermal Conductance over Wings. NACA ARR, March 1943.

9. Brunt, David: Physical and Dynamical Meteorology. Univ. Press (Cambridge), 2d ed., 2d reprint, 1944, fig. 17, p. 61.

10. Hardy, J. K.: Kinetic Temperature of Wet Surfaces. A Method of Calculating the Amount of Alcohol Required to Prevent Ice, and the Derivation of the Psychrometric Equation. NACA ARR No. 5G13, 1945.

11. Boelter, L. M. K., Martinelli, R. C., Romie, F. E., and Morrin, E. H.: An Investigation of Aircraft Heaters. XVIII - A Design Manual for Exhaust Gas and Air Heat Exchangers. NACA ARR No. 5A06, 1945.

12. Dodge, Russell A., and Thompson, Milton J.: Fluid Mechanics. McGraw-Hill Book Co., Inc., 1937, pp. 204-207.

13. von Kármán, Th., and Milliken, C. B.: On the Theory of Laminar Boundary Layers Involving Separation. NACA Rep. No. 504, 1934.

14. von Doenhoff, Albert E.: A Method of Rapidly Estimating the Position of the Laminar Separation Point. NACA TN No. 671, 1938.

15. Emmons, Howard W.: The Numerical Solution of Partial Differential Equations. Quarterly Appl. Math., vol. II, no. 3, Oct. 1944, pp. 173-195.

16. Squire, H. B.: Heat Transfer Calculation for Aerofoils. R. & M. No. 1986, British A.R.C., 1942.

17. Seibert, Otto: Heat Transfer of Airfoils and Plates. NACA TM No. 1044, 1943.

18. Schmidt, Ernst, and Wenner, Karl: Heat Transfer over the Circumference of a Heated Cylinder in Transverse Flow. NACA TM No. 1050. 1943.

19. Hardy, J. K.: An Analysis of the Dissipation of Heat in Conditions of Icing from a Section of the Wing of the C-46 Airplane. NACA ARR No. 4I11a, 1944.

TABLE I - PROPELLER DATA

Station	24	36	48	60
Blade radius, r, ft	2	3	4	5
Blade-segment radial length, l, ft	1	1	1	1
Blade chord, c, ft	1.05	1.06	1.07	0.986
Equivalent leading-edge cylinder diameter, D_c, ft	0.027	0.0095	0.0057	0.0040
External heat-transfer area, A_a, sq ft	1.26	1.18	1.15	1.06
Internal heat-transfer area, A_g, sq ft	1.13	1.05	1.01	0.942
Internal blade-passage perimeter, P, ft	1.13	1.05	1.01	0.942
Internal blade-passage cross-sectional area, A_p, sq ft	0.0558	0.0315	0.0239	0.0173
Internal blade passage cross-sectional area at point 1, $A_{p,1}$, sq ft	0.0875	0.0375	0.0275	0.0205
Internal blade passage cross-sectional area at point 2, $A_{p,2}$, sq ft	0.0375	0.0275	0.0205	0.0141

TABLE II - CALCULATED DATA FOR NUMERICAL EXAMPLES

	Condition A				Condition B			
Station	24	36	48	60	24	36	48	60
Blade-section lift coefficient, C_l	0.413	0.550	0.583	0.474	0.570	0.597	0.553	0.436
Blade-section angle of attack, α, deg	2.6	2.8	2.9	2.3	5.0	3.2	2.4	1.7
Blade resultant velocity, V_R, ft/sec	658	740	839	951	505	539	582	622
Mean internal radial gas velocity, $u_{r,m}$, ft/sec	88.0	145.8	175.5	217.5	159.6	274.5	345.9	465.5
Friction flow energy, F_{1-2}, ft-lb/lb	15.7	69.4	124.8	239.9	46.0	216.4	425.9	966.3
Blade-metal heat transfer, Q_{trans}, Btu/hr	3726	5293	6070	6280	5404	7920	8540	8674
Polytropic specific heat, c_n, Btu/(lb)(^oF)	0.2941	0.3028	0.3157	0.3285	0.2275	0.2351	0.2264	0.1839
Polytropic exponent, n	0.441	0.478	0.525	0.563	-0.223	-0.077	-0.247	-4.51

NATIONAL ADVISORY COMMITTEE
FOR AERONAUTICS

Station	24	36	48	60	24	36	48	60
Propeller enthalpy increment, W_{prop}, ft-lb/lb	1400	2100	2800	3500	438	656	874	1092
Radial kinetic-energy change of internal gas, E_{1-2}, ft-lb/lb	202.0	147.9	188.0	401.3	698	608	955	2575
Tip-nozzle heat escape, Q_n, Btu/hr	35,250				59,200			
Summation of blade-metal heat transfer, ΣQ_{trans}, Btu/hr	21,369				30,538			
Effectiveness of blade as heat exchanger	0.379				0.341			

NATIONAL ADVISORY COMMITTEE
FOR AERONAUTICS

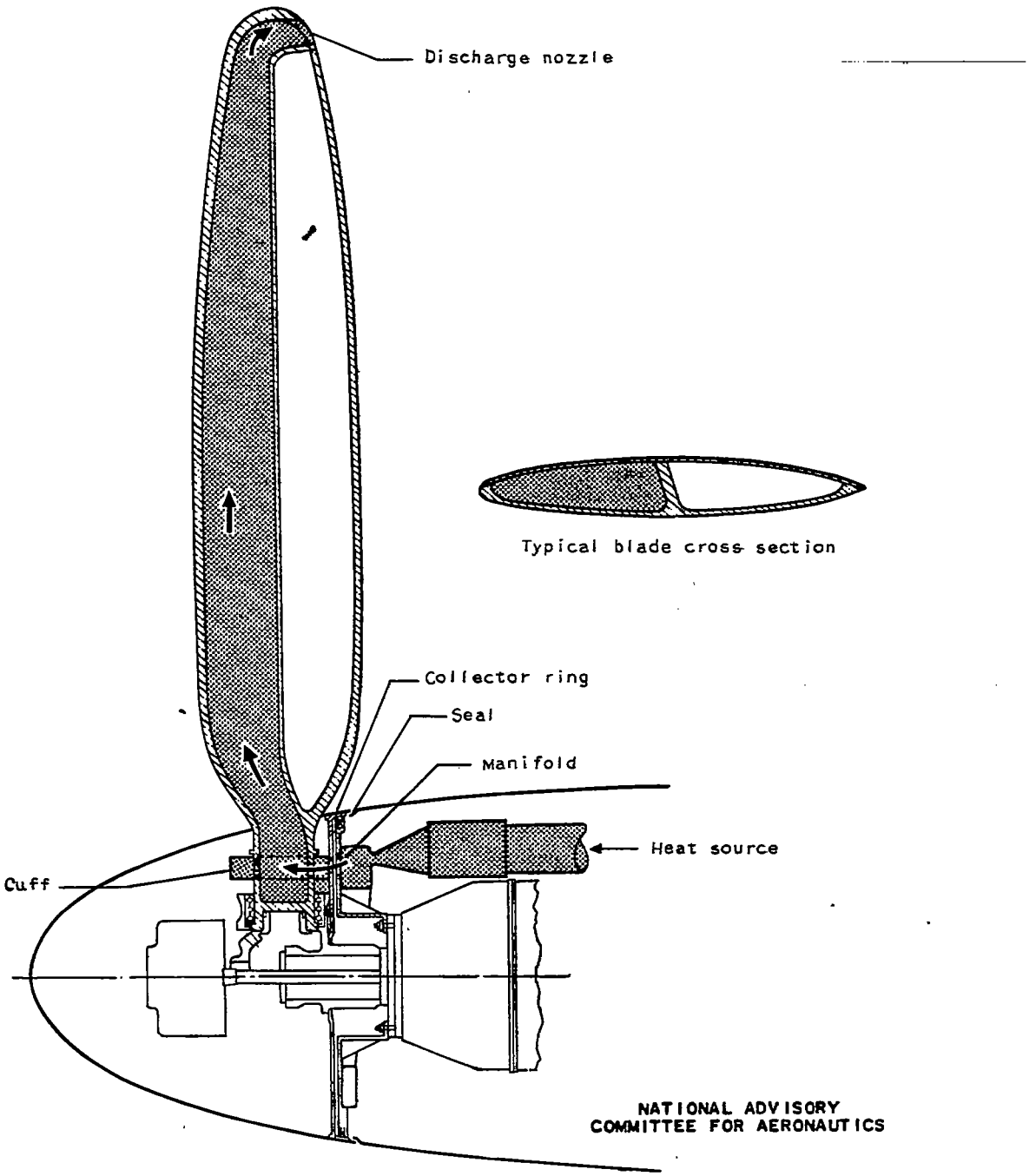

Figure 1. - Schematic flow diagram for gas-heated hollow propeller blade.

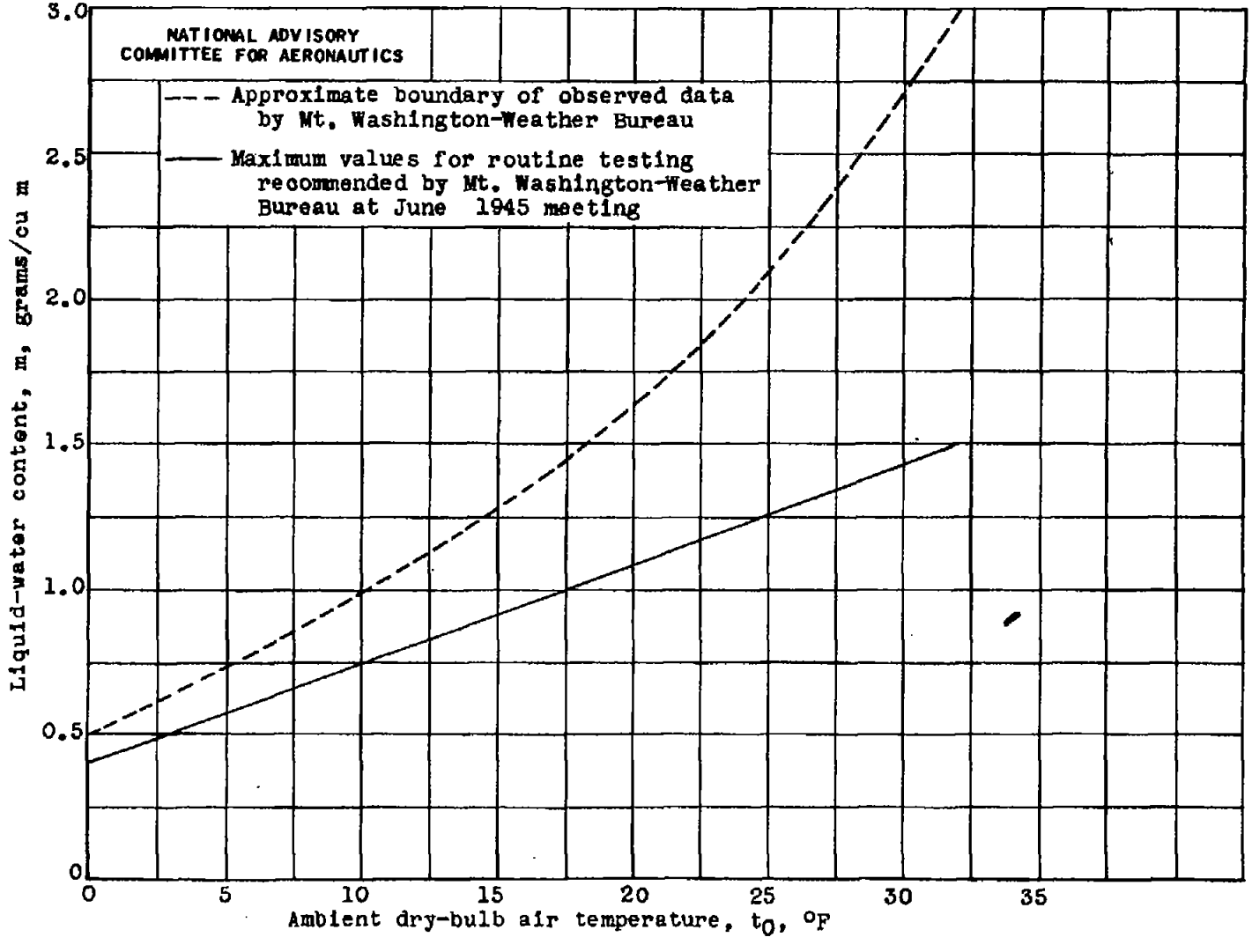

Figure 2. - Variation of liquid-water content with temperature.

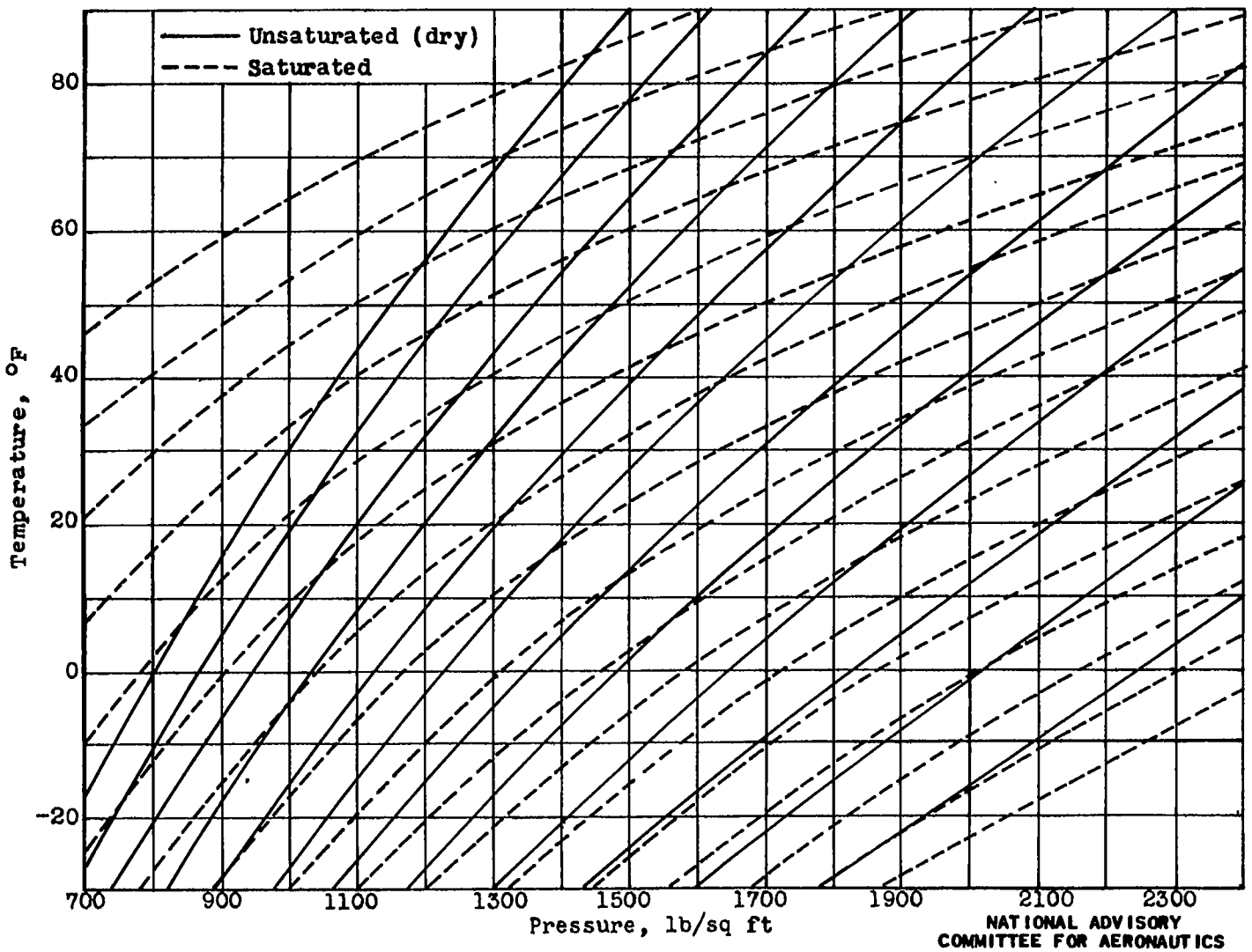

Figure 3. - Adiabatic temperature and pressure chart for saturated and unsaturated air. (Data from reference 9.)

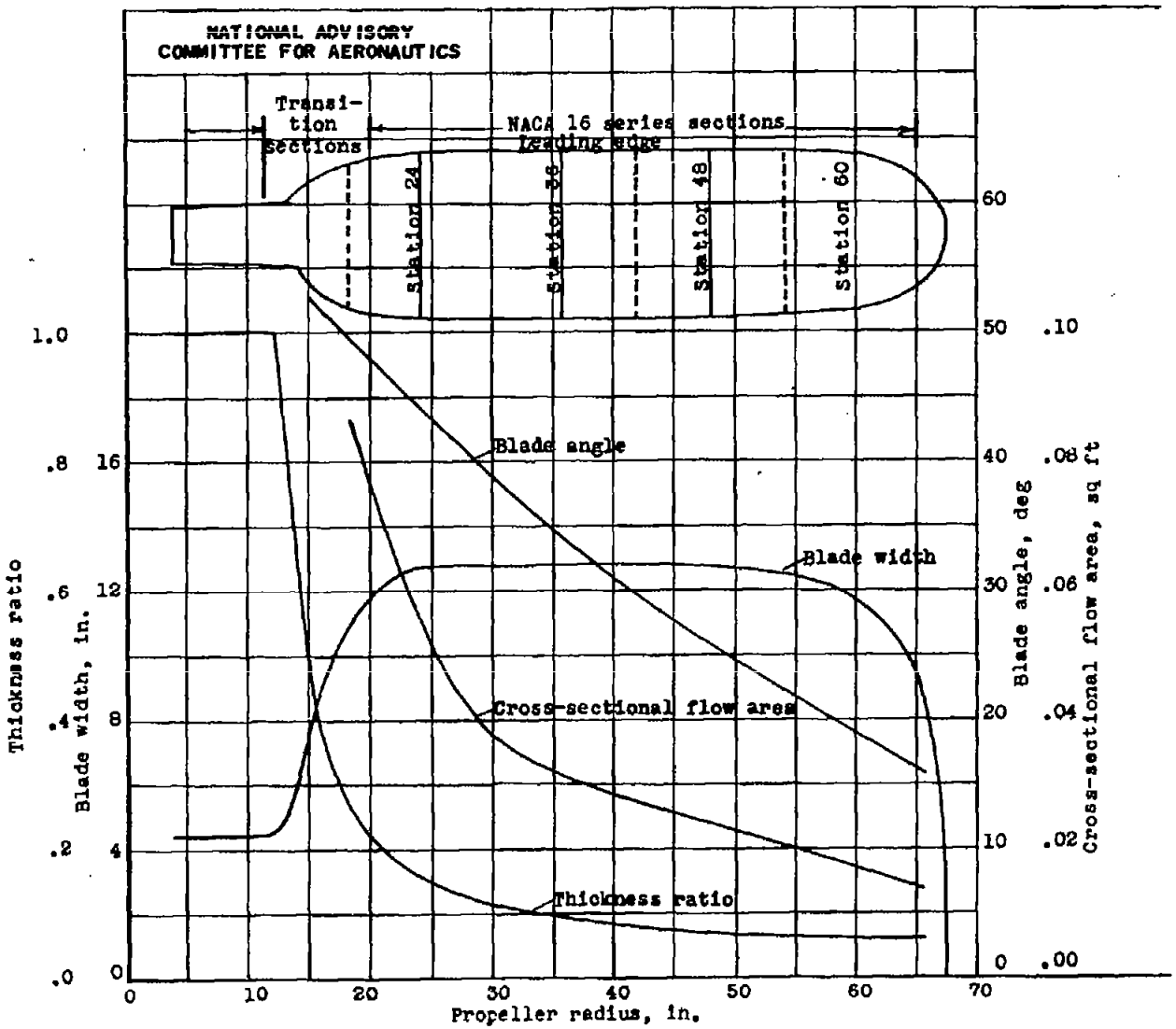

Figure 4. - Propeller-blade-form characteristics.

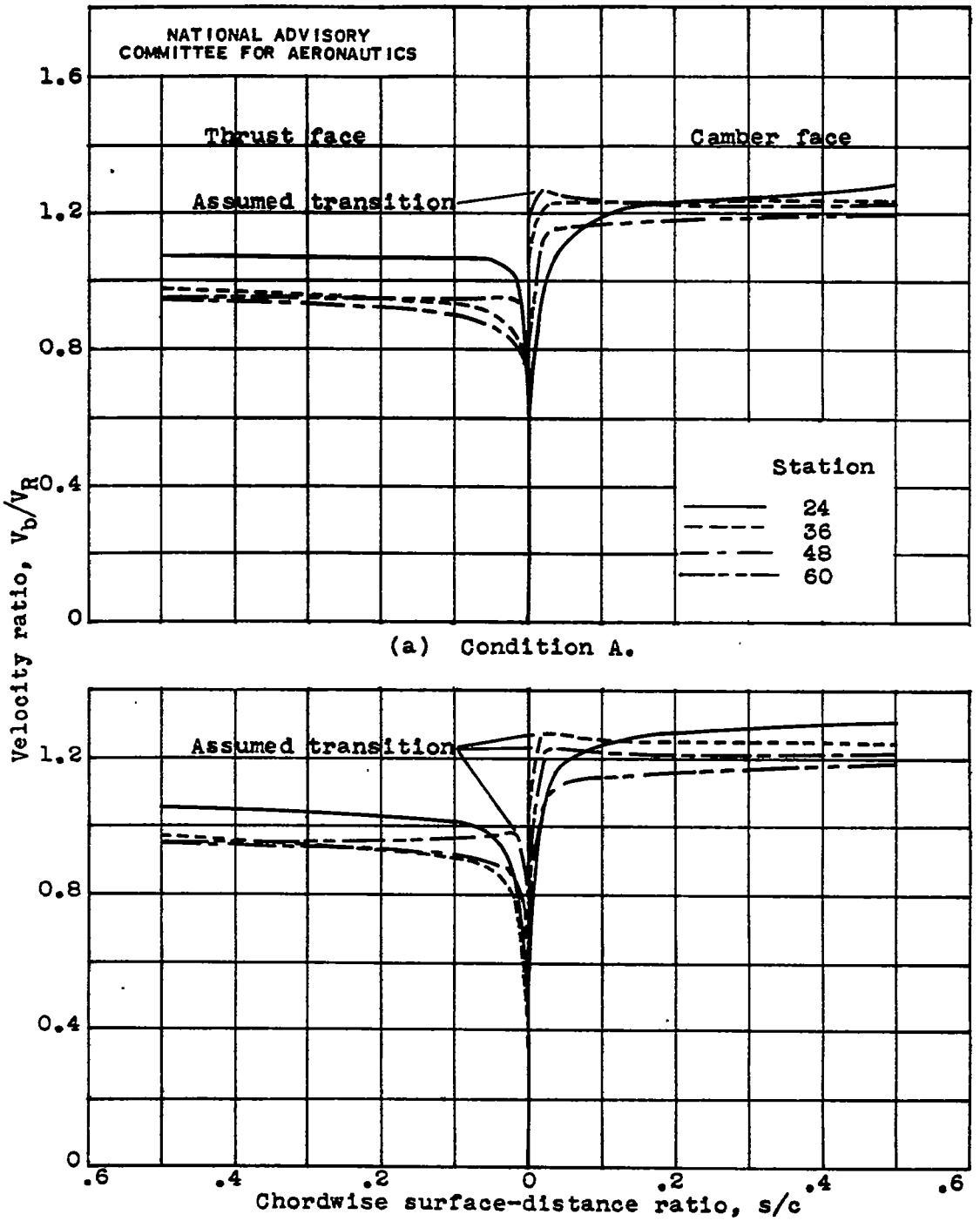

Figure 5. - Chordwise variation of local velocity ratio for two conditions.

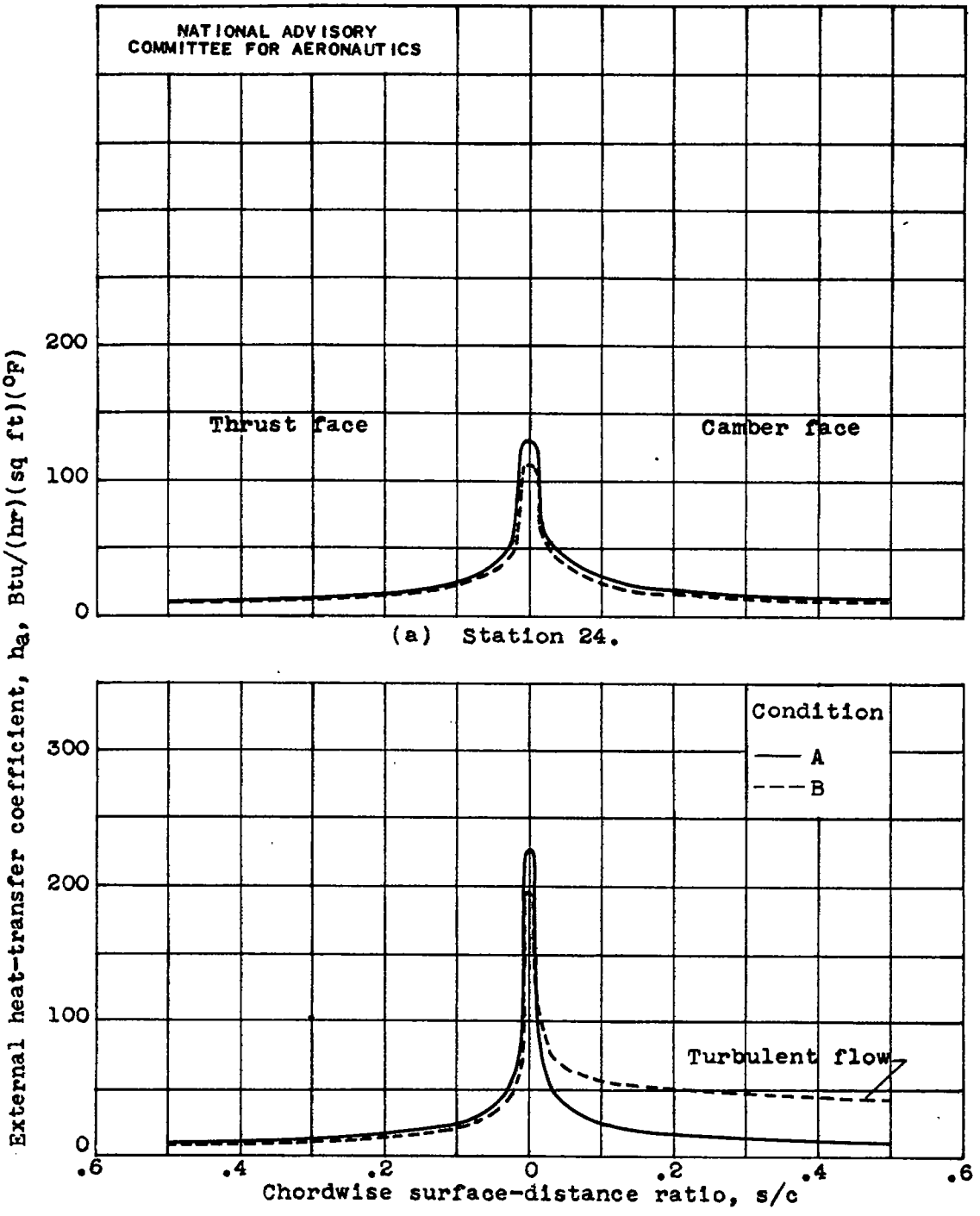

Figure 6. - Chordwise variation of external heat-transfer coefficient for two conditions.

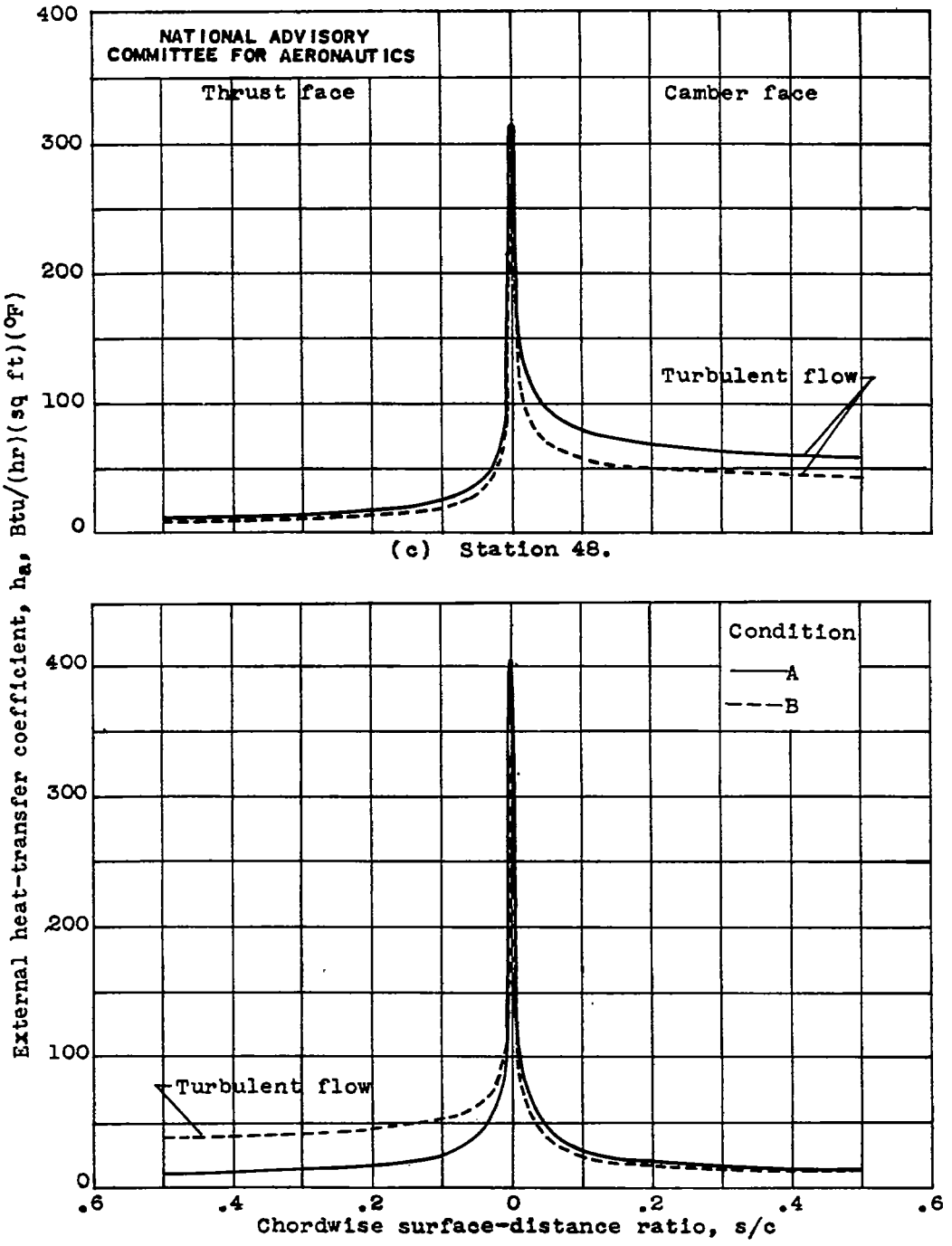

Figure 6. - Concluded. Chordwise variation of external heat-transfer coefficient for two conditions.

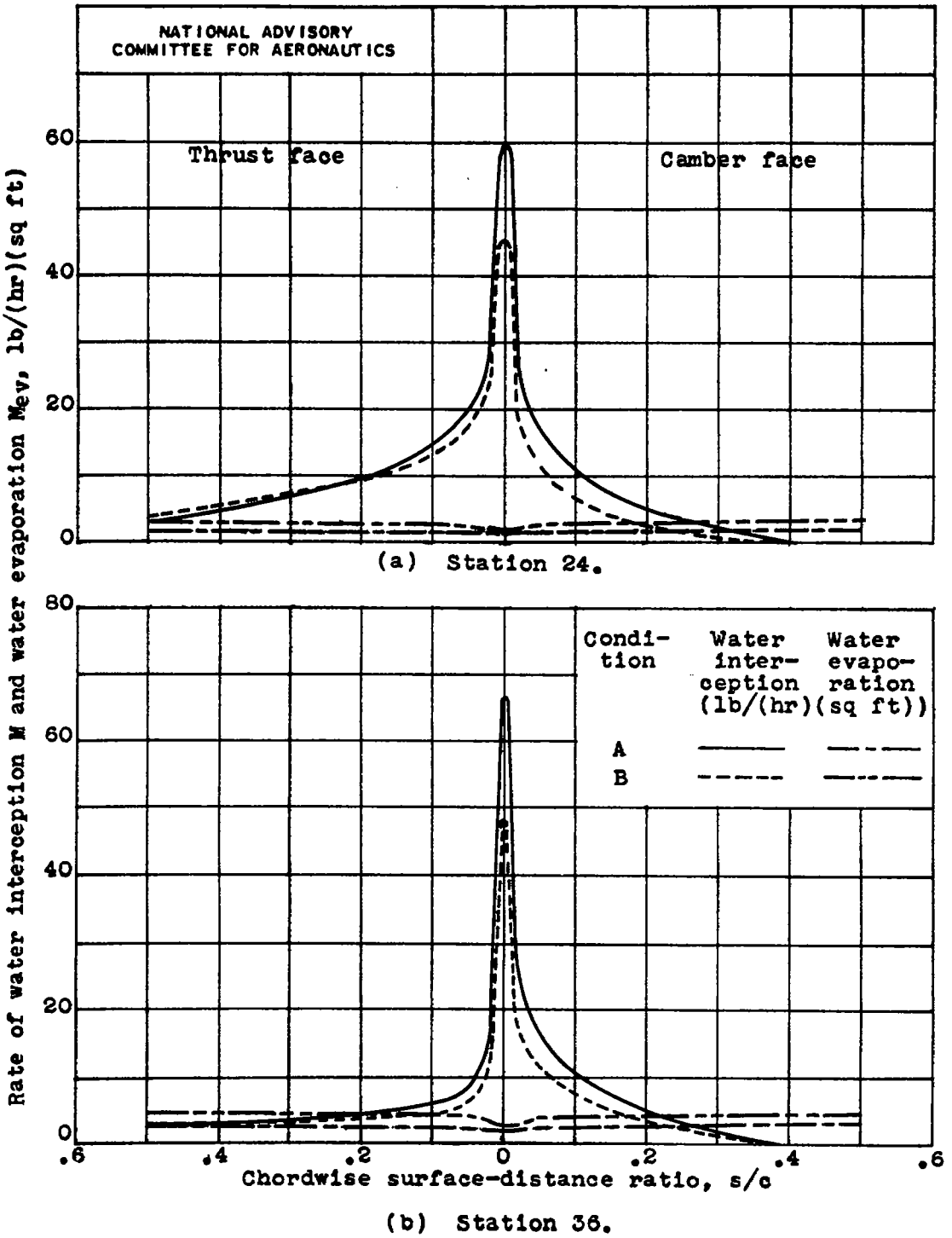

Figure 7. - Chordwise variation of rates of water interception and water evaporation for two conditions.

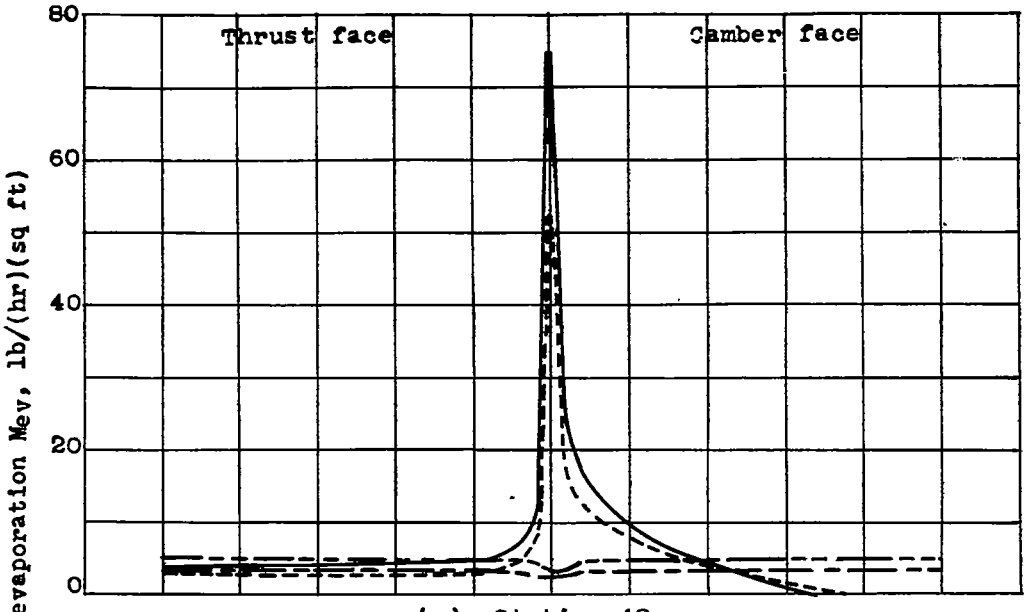

(c) Station 48.

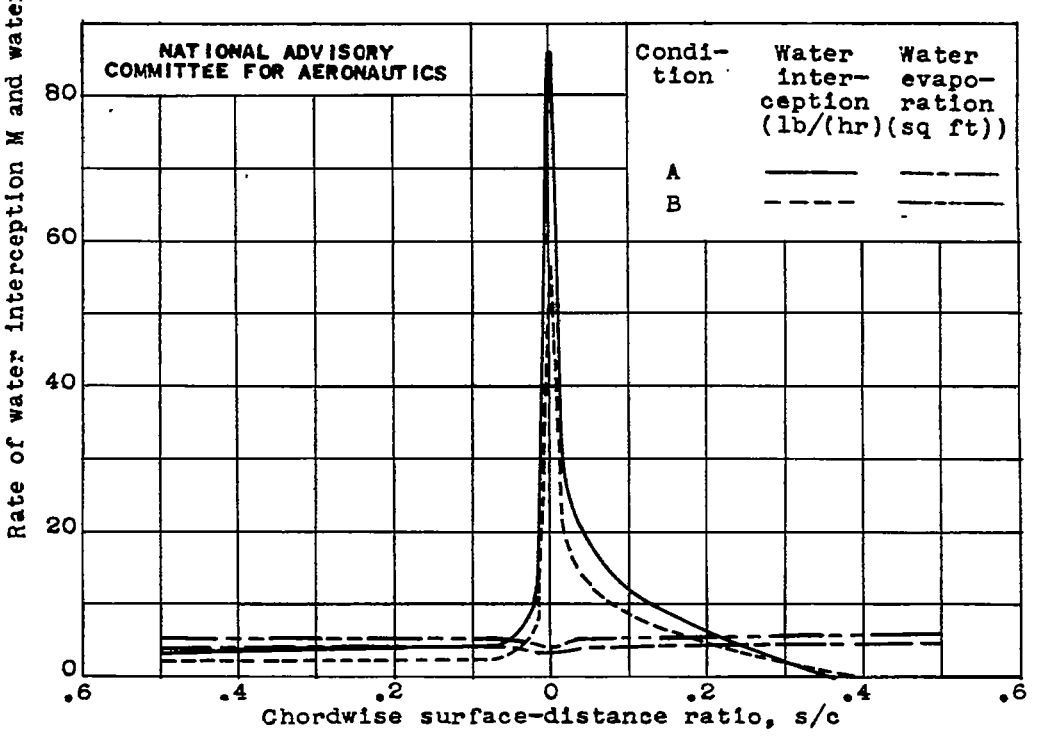

(d) Station 60.

Figure 7. - Concluded. Chordwise variation of rates of water interception and water evaporation for two conditions.

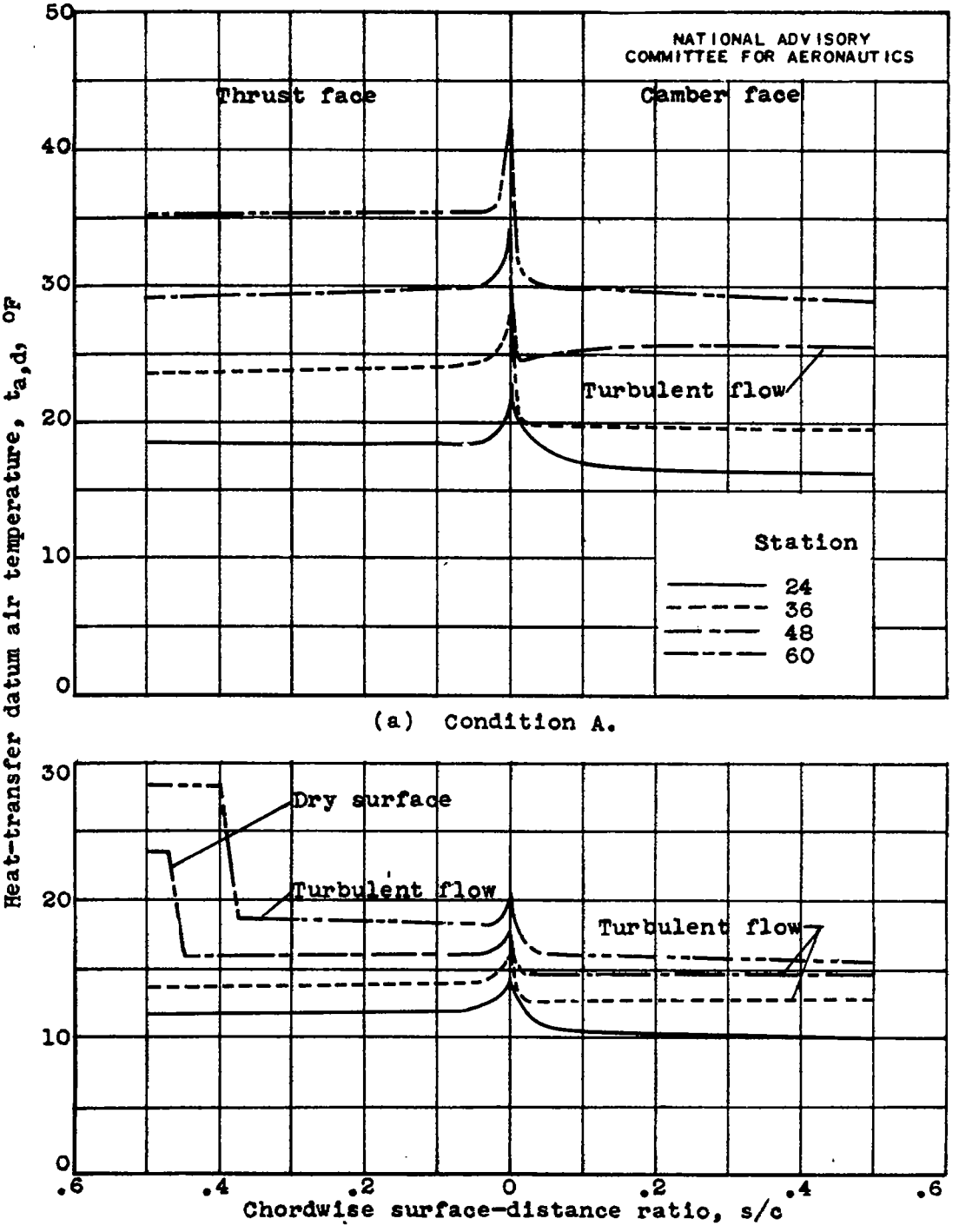

Figure 8. - Chordwise variation of heat-transfer datum air temperature for two conditions.

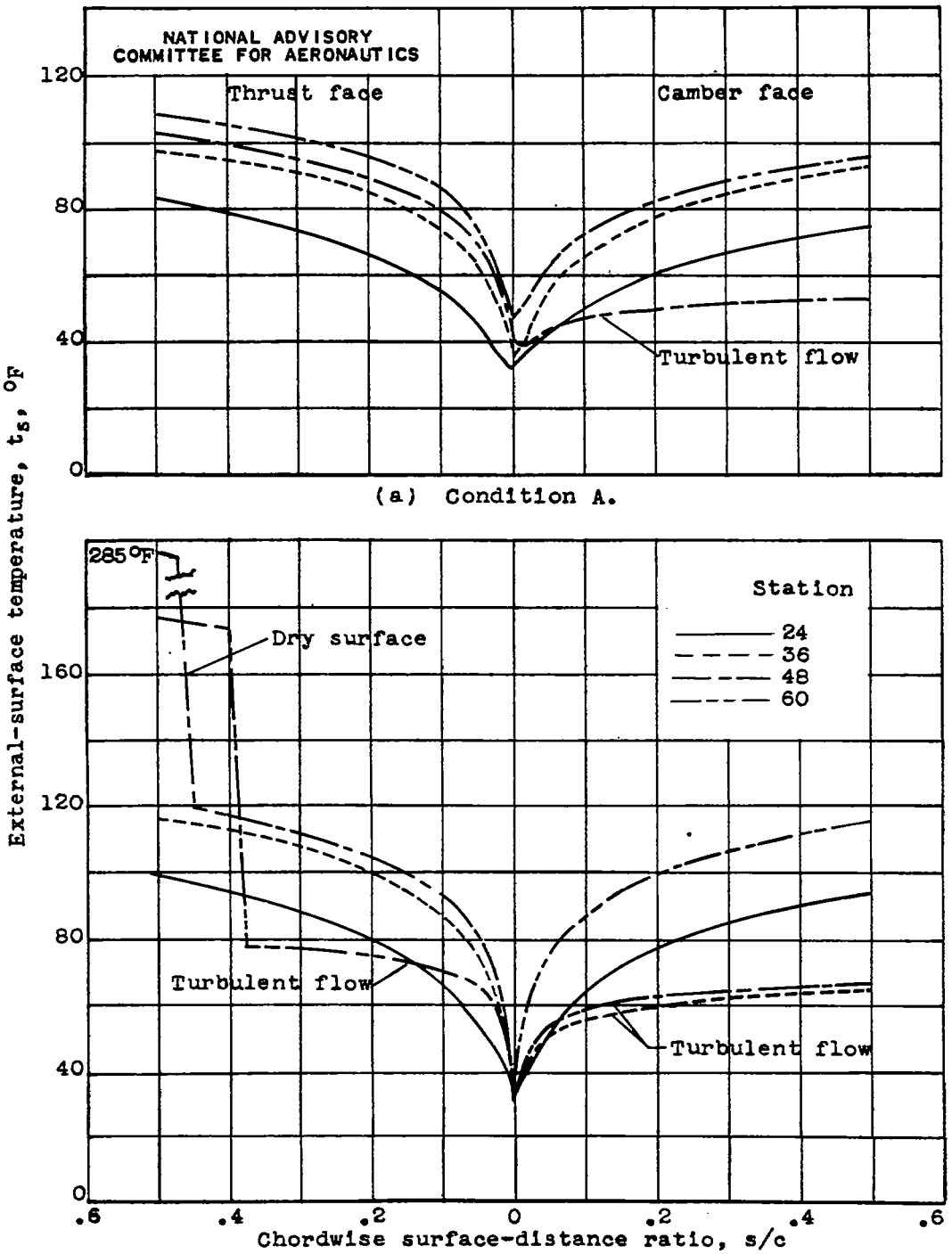

Figure 9. - Chordwise variation of external-surface temperature for two conditions.

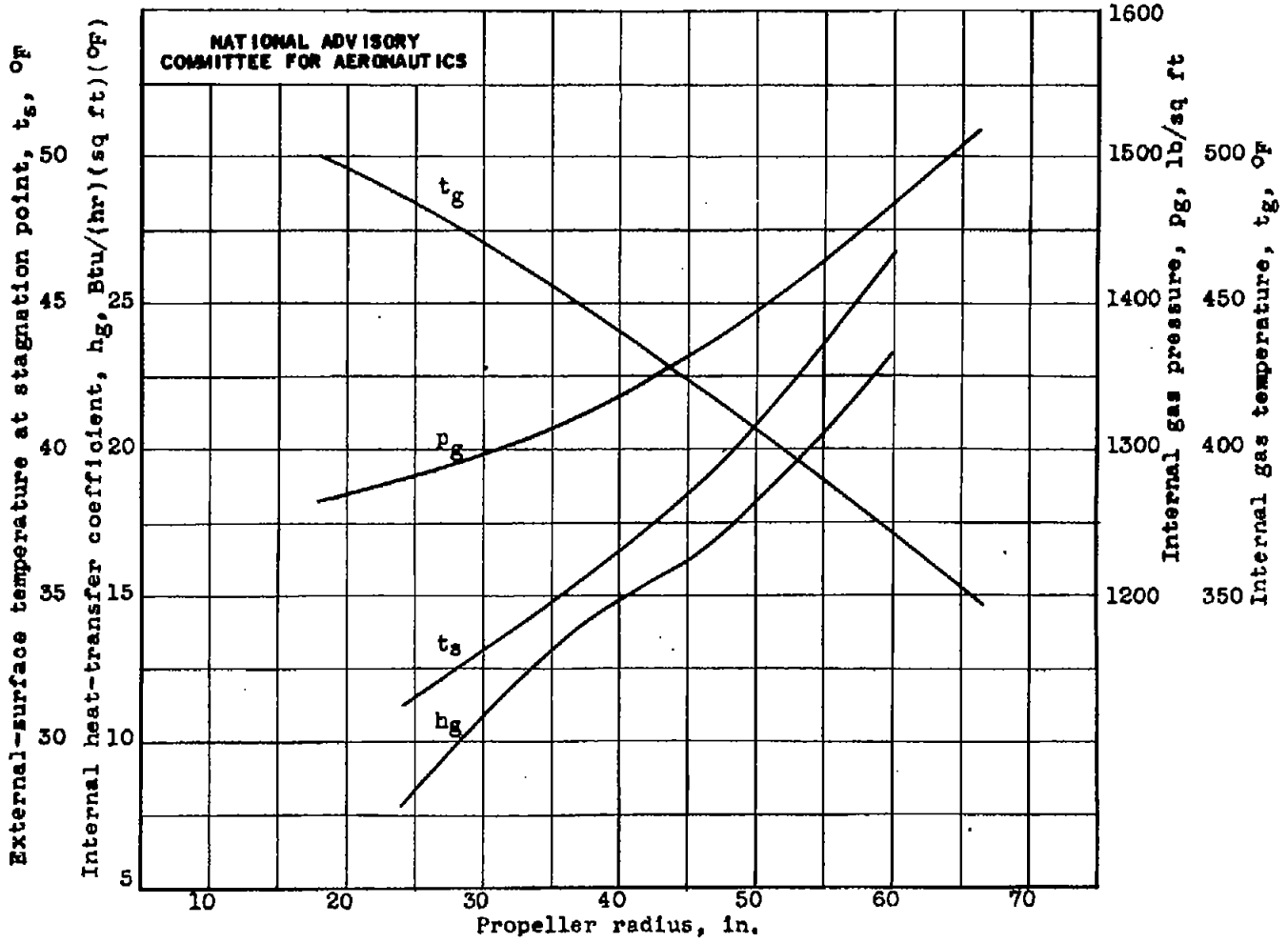

(a) Condition A.

Figure 10. - Radial variation of internal gas temperature, internal gas pressure, internal heat-transfer coefficient, and external-surface temperature at stagnation point.

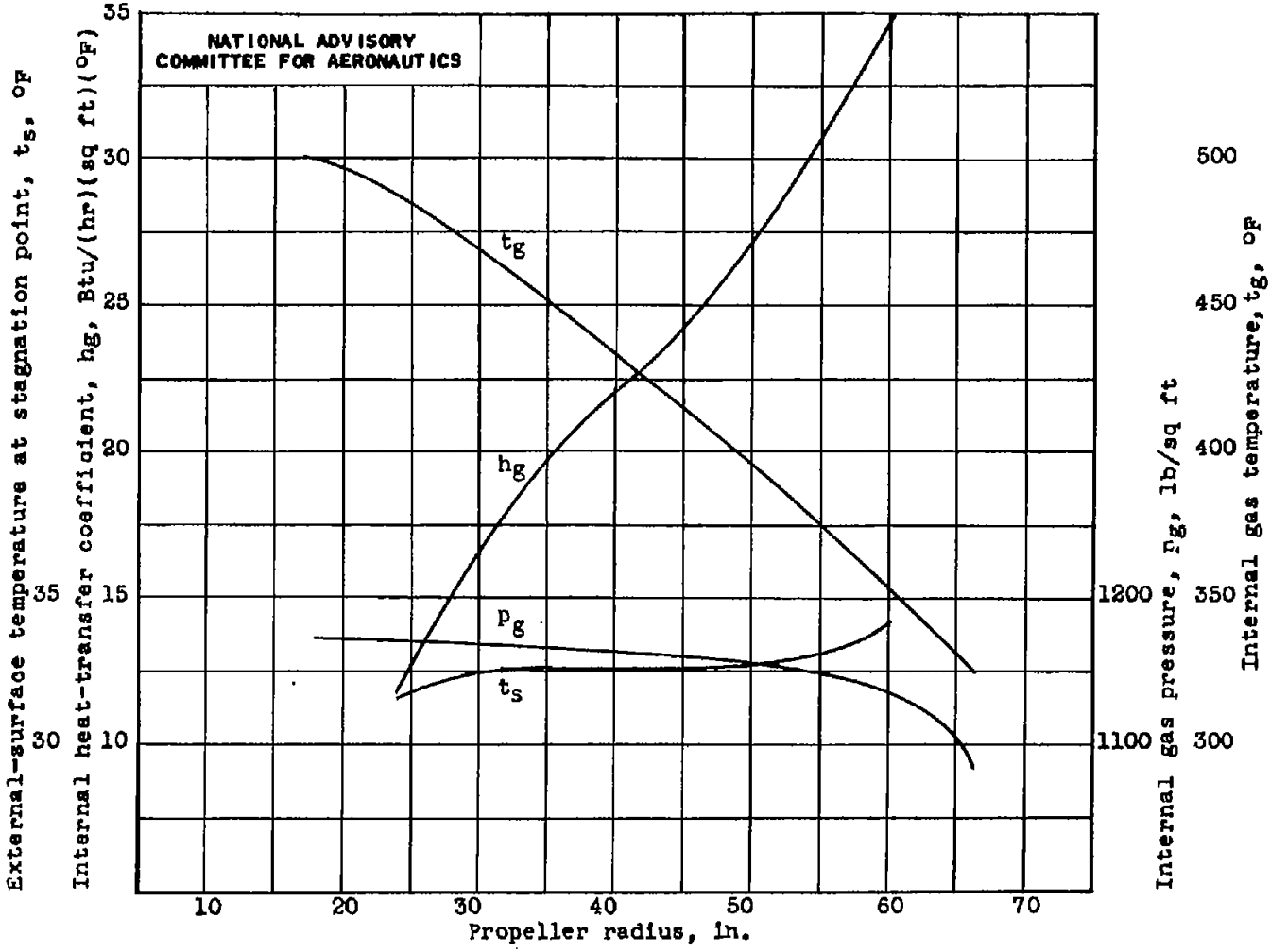

(b) Condition B.

Figure 10. - Concluded. Radial variation of internal gas temperature, internal gas pressure, internal heat-transfer coefficient, and external-surface temperature at stagnation point.

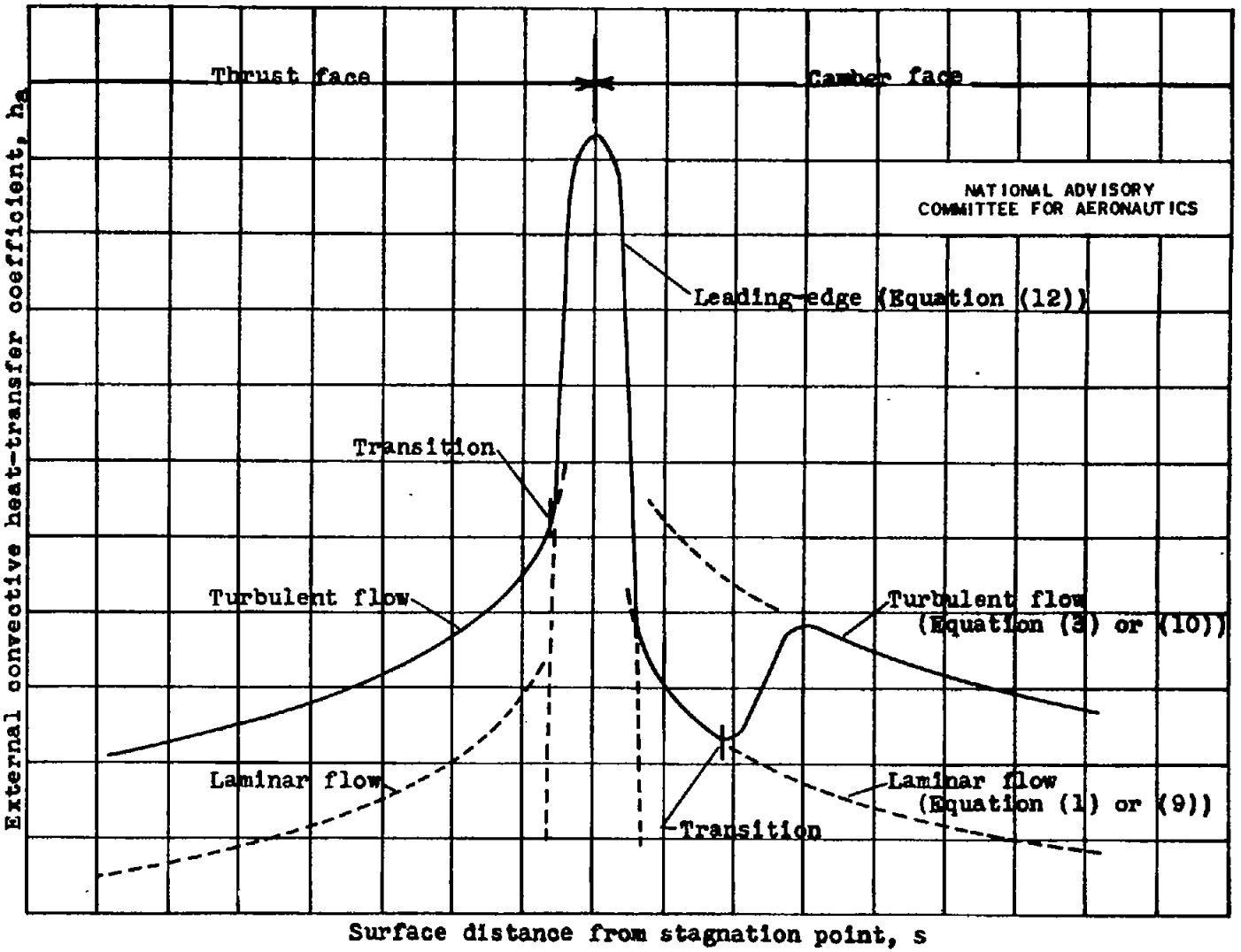

Figure 11. - Diagram of typical chordwise variation of external heat-transfer coefficient over propeller blade.

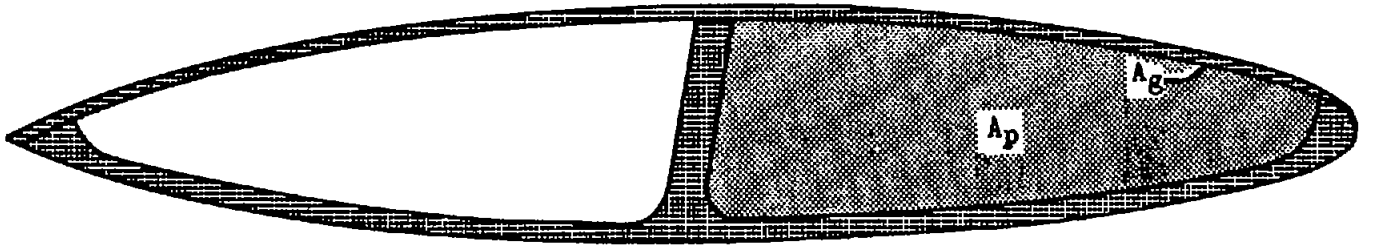

(a) Original blade section

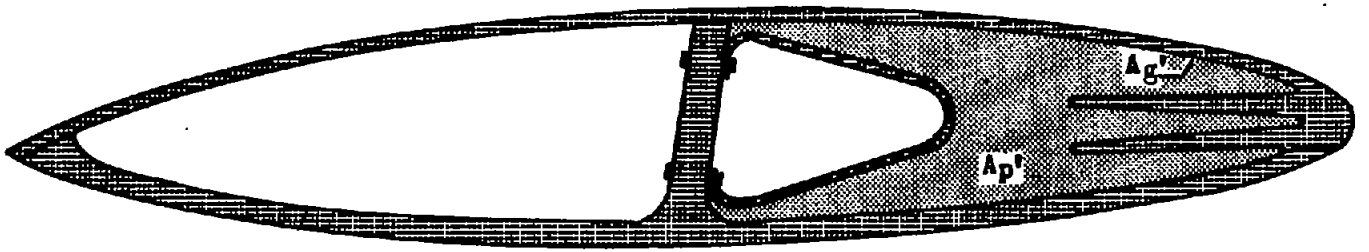

(b) Modification 1: Cross-sectional flow area ratio, $A_p/A_p' = 2$; internal heat-transfer area ratio, $A_g'/A_g = 2$.

NATIONAL ADVISORY
COMMITTEE FOR AERONAUTICS

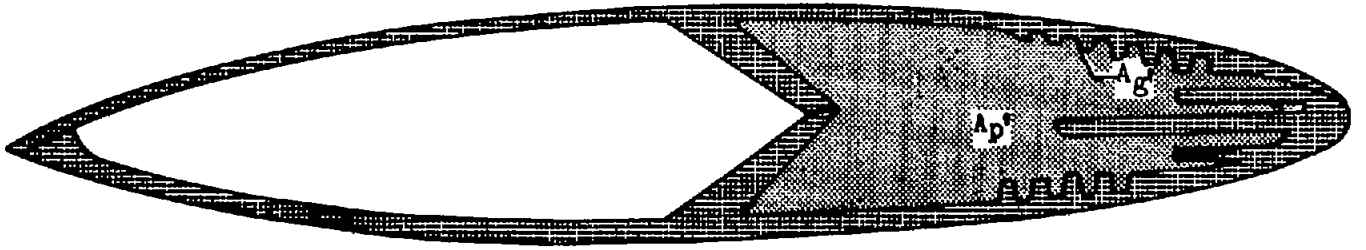

(c) Modification 2: Cross-sectional flow area ratio, $A_p/A_p' = 1.5$; internal heat-transfer area ratio, $A_g'/A_g = 2.5$.

Figure 12. - Comparison of original with two propeller-blade-section modifications that indicate savings in internal heat flow.

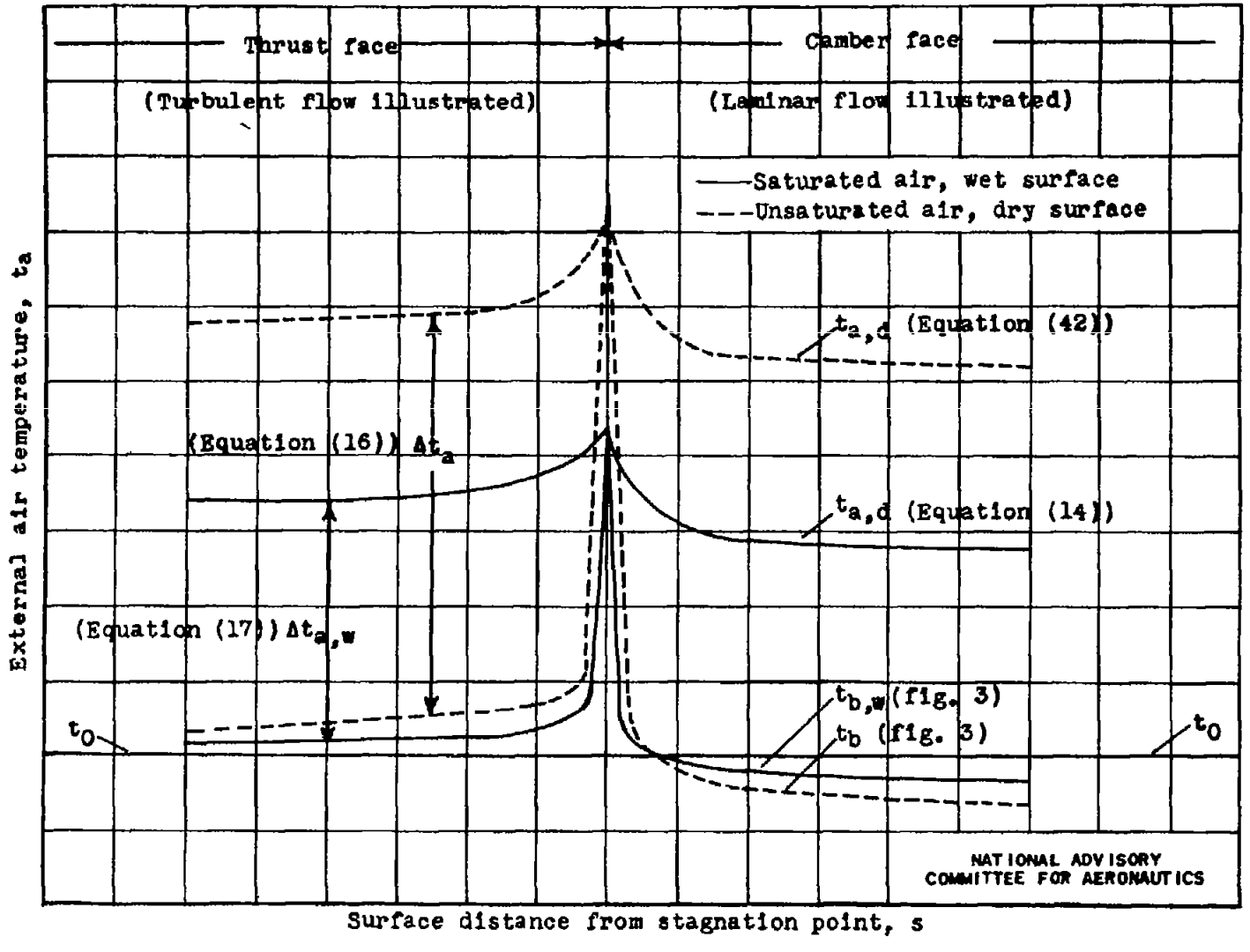

Figure 13. - Diagram of typical chordwise variation of heat-transfer datum temperature.

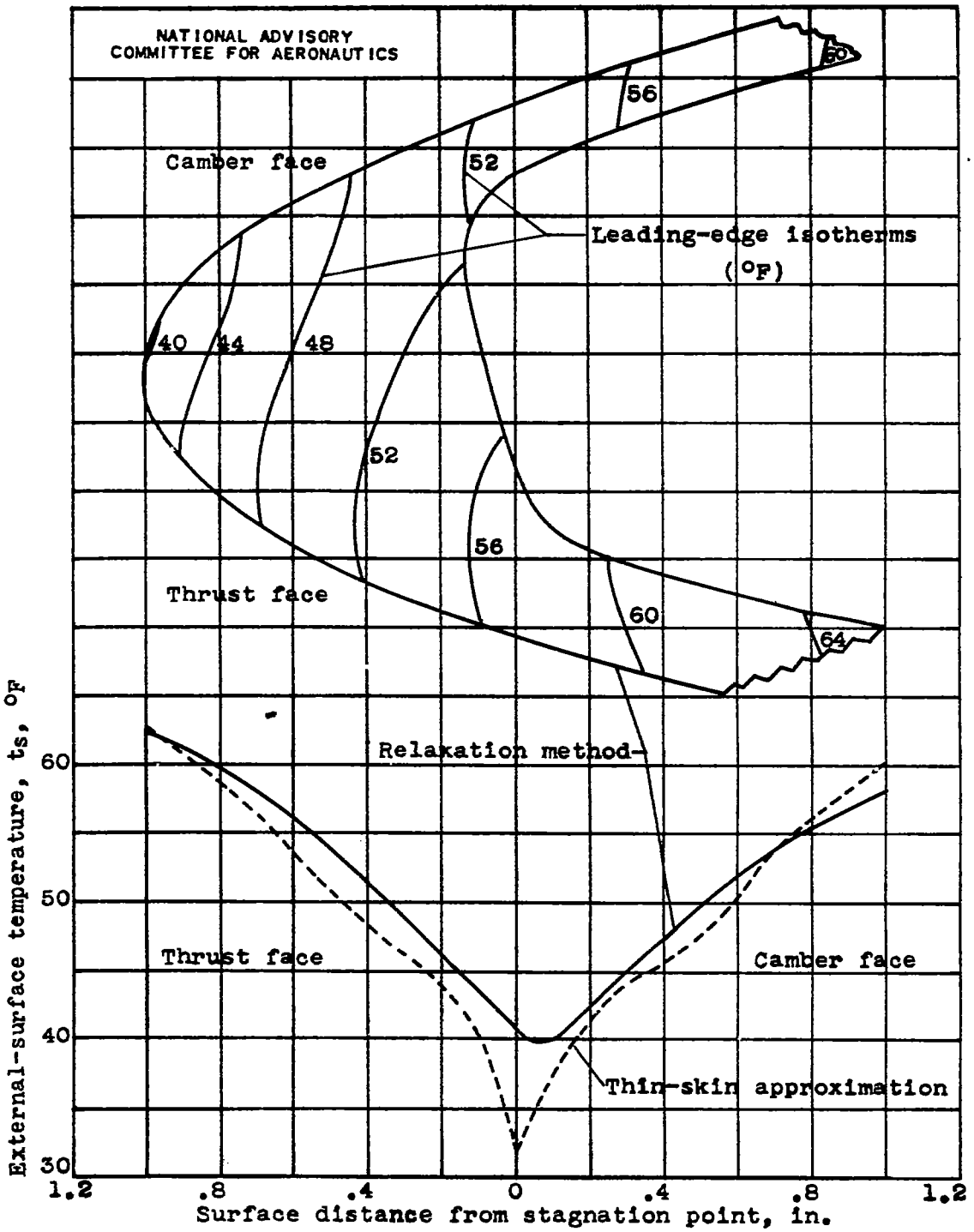

Figure 14. - Comparison of leading-edge surface temperature by two methods for station 24, condition B.